

# FL-MedSegBench: A Comprehensive Benchmark for Federated Learning on Medical Image Segmentation

Meilu Zhu, Zhiwei Wang, Axiu Mao, Yuxing Li, Xiaohan Xing, Yixuan Yuan, Edmund Y. Lam\*

**Abstract**—Federated learning (FL) offers a privacy-preserving paradigm for collaborative medical image analysis without sharing raw data. However, the absence of standardized benchmarks for medical image segmentation hinders fair and comprehensive evaluation of FL methods. To address this gap, we introduce **FL-MedSegBench**, the first comprehensive benchmark for federated learning on medical image segmentation. Our benchmark encompasses nine segmentation tasks across ten imaging modalities, covering both 2D and 3D formats with realistic clinical heterogeneity. We systematically evaluate eight generic FL (gFL) and five personalized FL (pFL) methods across multiple dimensions: segmentation accuracy, fairness, communication efficiency, convergence behavior, and generalization to unseen domains. Extensive experiments reveal several key insights: (i) pFL methods, particularly those with client-specific batch normalization (e.g., FedBN), consistently outperform generic approaches; (ii) No single method universally dominates, with performance being dataset-dependent; (iii) Communication frequency analysis shows normalization-based personalization methods exhibit remarkable robustness to reduced communication frequency; (iv) Fairness evaluation identifies methods like Ditto and FedRDN that protect underperforming clients; (v) A method’s generalization to unseen domains is strongly tied to its ability to perform well across participating clients. We will release an open-source toolkit to foster reproducible research and accelerate clinically applicable FL solutions, providing empirically grounded guidelines for real-world clinical deployment. The source code is available at <https://github.com/meiluzhu/FL-MedSegBench>.

**Index Terms**—Medical Image Segmentation, Benchmark, Federated Learning, Personalized Federated Learning.

## I. INTRODUCTION

Medical image segmentation [1]–[4] plays a vital role in clinical decision-making, enabling precise localization of anatomical structures and pathological regions. Deep learning models have achieved remarkable success in this domain [5], [6]. However, their training typically relies on large and centralized datasets—a requirement that directly conflicts with patient privacy regulations (e.g., HIPAA [7], GDPR [8]) and the inherently distributed nature of medical data across hospitals and institutions [9], [10]. Federated learning (FL) has

emerged as a privacy-preserving alternative, allowing multiple institutions to collaboratively train models without exchanging local data [9], [11]–[14]. However, data from different sites exhibit inherent heterogeneity due to differences in imaging protocols, device manufacturers, patient populations, and clinical practices [15], [16]. It poses significant challenges to the convergence and generalization of FL models on segmentation tasks [17]–[19].

Pioneering FL researchers devoted substantial efforts to develop a global model that performs effectively across all participating clients [9]. These works, often categorized under generic Federated Learning (gFL), mainly focus on regularizing local training to align client objectives [15], [20], designing advanced server-side aggregation rules to improve global model fusion [21]–[24], and reducing domain shift with data augmentation [25]. Considering that a single shared global model cannot perform optimally for all clients simultaneously, personalized FL (pFL) has been gaining increasing popularity, which allows each client to learn client-specific models to adapt to local data [26]–[29]. Existing pFL approaches can be broadly categorized into: parameter decoupling (sharing base layers while personalizing higher layers) [30], [31], model interpolation (mixing global and local models) [32] and batch normalization layer personalization [33], [34]. The overarching goal of pFL is to balance generalization and specialization, thereby achieving superior performance on heterogeneous local data distributions.

Though fruitful FL methods have been explored, a standardized benchmark for medical image segmentation is still lacking. As a result, current evaluations of FL methods in this domain suffer from the absence of standardized benchmarks and inconsistent implementations, leading to ambiguous conclusions regarding their effectiveness and robustness across diverse practical scenarios. Although two FL benchmarks [35], [36] have been proposed, they lack comprehensiveness in terms of data scale, task diversity, and modality coverage. For example, FLamby [35] only contains three 3D segmentation datasets (covering only two modalities) and does not evaluate pFL methods. Manthe et al. [36] built a benchmark only for brain tumor segmentation, lacking task and modality diversity.

To address these gaps, we introduce a comprehensive benchmark for federated medical image segmentation named **FL-MedSegBench**. As shown in Fig. 1, its data comes from **27 datasets** and covers **nine medical segmentation tasks** across **ten imaging modalities** and both **2D and 3D formats**. To faithfully reflect real-world scenarios, each task incorporates

This work described in this paper was fully supported by a grant (ITS/341/23) from the Innovation and Technology Fund of Hong Kong, China.

M. Zhu, Z. Wang, Y. Li, and Edmund Y. Lam are with Department of Electrical and Computer Engineering, The University of Hong Kong, Hong Kong, China; A. Mao is with School of Communication Engineering, Hangzhou Dianzi University, Hang Zhou, China; X. Xing is with Department of Radiation Oncology, Stanford University, California, USA; Y. Yuan is with Department of Electronic Engineering, Chinese University of Hong Kong, Hong Kong, China.

M. Zhu and Z. Wang contributed equally to this work. Edmund Y. Lam is the corresponding author (elam@eee.hku.hk).

data acquired from different institutions or imaging devices. These tasks include vessel segmentation with fundus images, meibomian gland segmentation with infrared images, adenocarcinoma detection with pathology images, polyp segmentation with endoscopic images, prostate segmentation with MRI slices, breast lesion segmentation with ultrasound images, right ventricle segmentation with CMR volumes, pancreas lesion segmentation with MRI-T1 scans and brain tumor segmentation using multi-modal MRI (four modalities). We evaluate **eight gFL** and **five pFL methods** under realistic non-IID data. Our benchmark assesses not only segmentation accuracy but also fairness, communication efficiency, convergence behavior, and generalization to unseen clients. Through extensive experiments, we highlight the strengths and limitations of existing approaches and identify promising directions for future research. We hope this work will facilitate the development of more robust, efficient, and clinically applicable FL solutions for medical imaging. Our main contributions are listed as follows:

- 1) **A comprehensive and curated collection of medical segmentation datasets for FL research.** We collect data from 27 datasets covering nine medical segmentation tasks spanning ten imaging modalities and covering both 2D and 3D formats. To facilitate realistic FL evaluation, we provide standardized data partitions with realistic non-IID distributions that mimic real-world clinical heterogeneity across institutions or devices.
- 2) **The first systematic benchmark for gFL and pFL in medical image segmentation.** We evaluate eight gFL methods (*e.g.*, FedAvg and FedProx) and five pFL methods (*e.g.*, FedBN and Ditto) across all nine datasets. The benchmark supports diverse evaluation dimensions including segmentation accuracy, fairness across clients, communication efficiency, convergence behavior, and generalization to unseen clients, providing a holistic view of method performance.
- 3) **Extensive experimental analysis under realistic FL scenarios.** We conduct rigorous experiments across nine medical segmentation tasks. Our analysis reveals several key insights into method performance, communication-computation trade-offs, fairness characteristics, and out-of-distribution generalization vulnerabilities. These findings provide empirically grounded guidance for selecting and deploying FL methods in real-world medical scenes.
- 4) **An open-source, modular, and extensible benchmark toolkit.** We release a fully reproducible codebase built on a modular FL framework, enabling easy integration of new datasets, models, and algorithms. The toolkit includes containerized environments, hyperparameter search scripts, and evaluation pipelines to ensure reproducibility and facilitate future research in federated medical image analysis.

**Roadmap.** The rest of the paper is organized as follows. In Section II, we will introduce two learning paradigms: generic federated learning (gFL) and personalized federated learning (pFL). Section III details the proposed FL-MedSegBench. We present the segmentation performance, convergence behavior

and generalization performance in Section IV. We discuss the choices made as well as the limitations of the benchmark in Section V. Finally, the paper is closed with the conclusion in Section VI.

## II. BACKGROUND AND PROBLEM FORMULATION

This section introduces the fundamental concepts of federated learning (FL) in medical image analysis, with a focus on image segmentation tasks. We formally review two learning paradigms: generic federated learning (gFL) and personalized federated learning (pFL).

### A. Generic Federated Learning

Generic Federated Learning (gFL) aims to train a single global model that generalizes effectively on the collective data distribution across all participating clients. In the context of medical image segmentation, this paradigm assumes that data originating from different hospitals or institutions, despite exhibiting variability due to differences in imaging protocols, acquisition devices, or patient demographics, share consistent underlying anatomical and pathological characteristics.

Formally, let  $\mathcal{D} = \bigcup_{k=1}^K \mathcal{D}_k$  represent the union of all local datasets from  $K$  clients (*e.g.*, clinical sites), where  $\mathcal{D}_k = \{(x_i^k, y_i^k)\}_{i=1}^{N_k}$  denotes the local dataset of the client  $k$  with  $N_k$  samples. Here,  $x_i^k \in \mathbb{R}^{H \times W \times D}$  is a training sample (*e.g.*, a 2D ultrasound image or 3D MRI scan), and  $y_i^k \in \{0, 1\}^{H \times W \times C}$  is the corresponding segmentation mask with  $C$  anatomical structures of interest. The objective of the gFL paradigm is to find a global segmentation model parameterized by  $W_g$  that minimizes the aggregate empirical risk:

$$\min_{W_g} \mathcal{F}(W_g) = \sum_{k=1}^K \alpha_k \mathcal{L}_k(W_g), \quad (1)$$

where  $\alpha_k$  is the aggregation weight of the  $k$ -th client.  $\mathcal{L}_k(W_g)$  is the local loss function for the client  $k$ , typically defined for segmentation tasks as:

$$\mathcal{L}_k(W_g) = \frac{1}{N_k} \sum_{i=1}^{N_k} \ell_{\text{seg}}(f(x_i^k; W_g), y_i^k). \quad (2)$$

Here,  $f(\cdot; W_g)$  denotes the segmentation model (*e.g.*, U-Net), and  $\ell_{\text{seg}}$  combines per-pixel losses such as Dice loss and binary cross-entropy (BCE) loss:

$$\ell_{\text{seg}}(\hat{y}, y) = \lambda \cdot \ell_{\text{Dice}}(\hat{y}, y) + (1 - \lambda) \cdot \ell_{\text{BCE}}(\hat{y}, y), \quad (3)$$

where  $\hat{y}$  is the predicted segmentation map, and  $\lambda \in [0, 1]$  balances the two loss terms.

To optimize the objective in Eq. (1), the standard gFL method, FedAvg [9], performs an iterative training procedure through multiple rounds of communication between the clients and a central server. In each communication round  $t \in [T]$ , the server first broadcasts the current global model parameters  $W_g^{(t)}$  to all participating clients. Subsequently, each client performs  $E$  local epochs to minimize its empirical loss function  $\mathcal{L}_k$  using its private data  $\mathcal{D}_k$ . Upon completion of local updates, the refined model  $W_k^{(t)}$  is transmitted back to the server, which aggregates them via a weighted averaging scheme:

$$W_g^{(t+1)} = \sum_{k=1}^K \alpha_k W_k^{(t)}, \quad \text{where} \quad \alpha_k = \frac{N_k}{\sum_{k=1}^K N_k}. \quad (4)$$

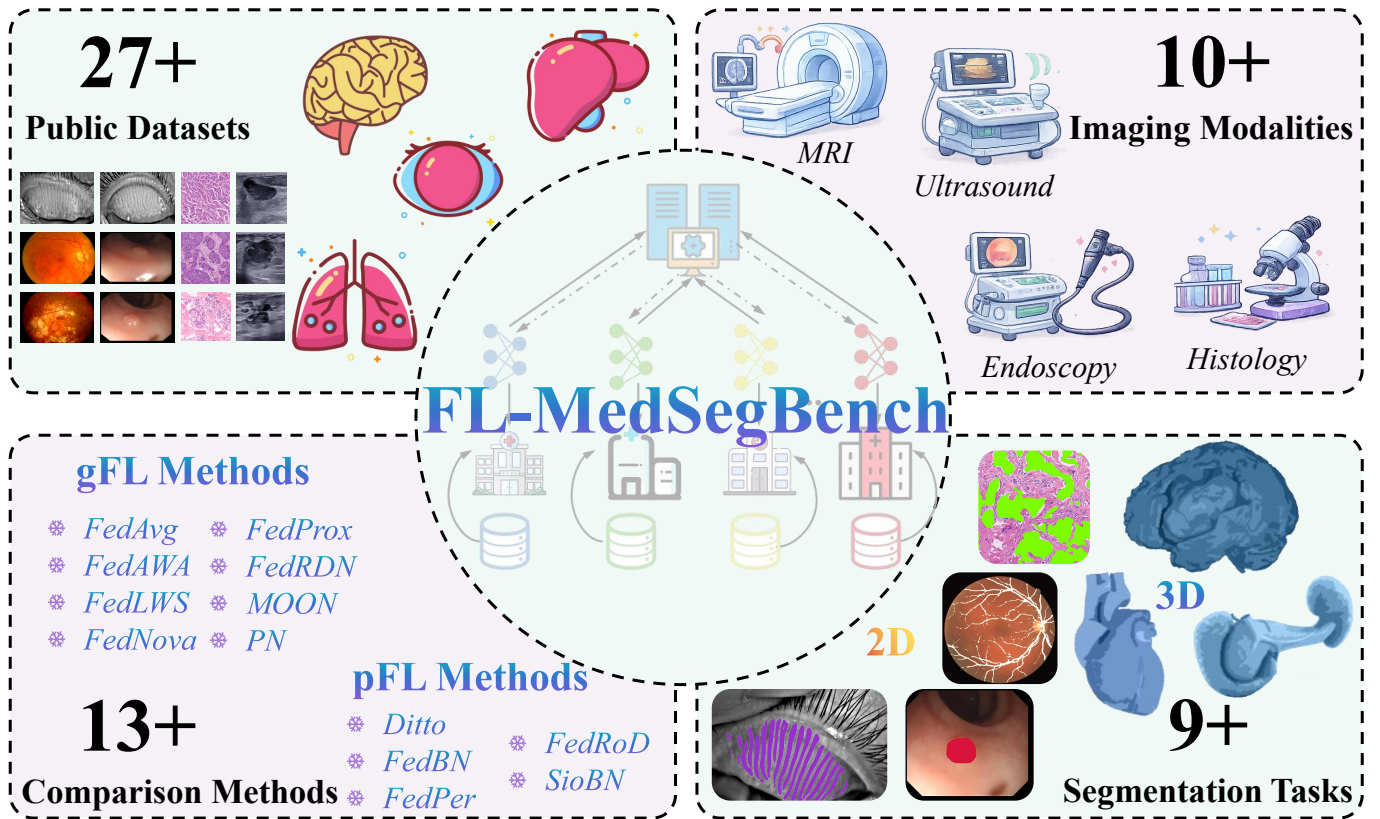


Fig. 1: FL-MedSegBench: a comprehensive benchmark for federated learning on medical image segmentation.

While FedAvg aims to produce a consensus model that performs uniformly across clients, its efficacy can degrade when local data distributions  $\mathcal{D}_k$  exhibit heterogeneity (*i.e.*, are non-IID), a prevalent challenge in medical imaging due to inter-institutional variability in acquisition protocols and patient populations. Many works have been proposed to improve FedAvg by introducing a regularization term to local training to align client objectives [15], [20], designing adaptive aggregation strategies [21]–[24], and reducing domain shift with data augmentation [25].

### B. Personalized Federated Learning

Personalized Federated Learning (pFL) addresses data heterogeneity by learning client-specific models  $\{W_k\}_{k=1}^K$  that are tailored to local data distributions while benefiting from collaborative training. In medical image segmentation, pFL is crucial when anatomical appearances, pathological patterns, or imaging protocols differ across institutions [37], [38].

The pFL objective is to balance local model adaptation and global knowledge sharing. Considering the absence of a universally agreed-upon objective function, we review existing methods and categorize their optimization objectives into two principal formulations [27], [28], [30]–[34], [39]. The first is defined as follows:

$$\min_{\{W_1, \dots, W_K\}} \sum_{k=1}^K \alpha_k \mathcal{L}_k(W_k) + \frac{\mu}{2} \mathcal{R}(W_g, W_1, \dots, W_K), \quad (5)$$

where  $\mathcal{R}(\cdot, \cdot)$  is a regularization term that encourages proximity between the local model  $W_k$  and a global reference model  $W_g$ , and  $\mu > 0$  controls the trade-off. A common choice of

$\mathcal{R}$  is applying an  $L_2$  regularizer between  $W_k$  and  $W_g$ . The corresponding local training step is generally formulated as

$$\mathcal{L}_k(W_k) = \frac{1}{N_k} \sum_{i=1}^{N_k} \ell_{\text{seg}}(f(x_i^k; W_k), y_i^k) + \frac{\mu}{2} \|W_k - W_g\|_2^2. \quad (6)$$

Here, the global model  $W_g$  is updated via Eq. (4). The regularizer term prevents local models from overfitting to small datasets and deviating excessively from the global consensus.

The second type of pFL methods generally decouples the model parameters into base layers  $W_B$  and personalized layers  $W_P$ . The base layers are jointly optimized by collaborating all clients while the personalized layers are updated locally and are not shared or aggregated with the server. The objective function of this type of pFL methods is formulated as

$$\min_{\{W_B, W_{(P,1)}, \dots, W_{(P,K)}\}} \sum_{k=1}^K \alpha_k \mathcal{L}_k(W_B, W_{(P,k)}). \quad (7)$$

The objective of the local training is defined as

$$\mathcal{L}_k(W_k) = \frac{1}{N_k} \sum_{i=1}^{N_k} \ell_{\text{seg}}(f(x_i^k; W_B, W_{(P,k)}), y_i^k). \quad (8)$$

Here, the base layers  $W_B$  are updated via Eq. (4). pFL has shown promise in medical image segmentation by improving accuracy on heterogeneous datasets while maintaining privacy.

## III. FL-MEDSEG BENCH

### A. Datasets

The experimental evaluation was conducted on a total of six 2D tasks (vessel, prostate, adenocarcinoma, breast tumor, meibomian gland, and polyp segmentation) and three 3D tasks (pancreas, right ventricular, and brain tumor segmentation).

TABLE I: Summary of the 2D medical datasets in FL-MedSegBench

Dataset	Index	Client Name	Sample size	Devices/Institutions
Fed-Vessel (Fundus)	C1	chaseDB [40]	28	Nidek NM-200-D
	C2	DR-Hagis [41]	40	Canon CR DGi/Topcon TRC-NW6s/Topcon TRC-NW8
	C3	DRIVE [42]	40	Canon CR5 nonmydriatic 3CCD/TopCon TRV-50
	C4	HRF [43]	45	Canon CF-60 UVi
	C5	LES-AV [44]	22	N/A
	C6	ORVS [45]	49	Zeiss, Visucam 200
Fed-Prostate (MRI-T2)	C1	RUNMC	411	Siemens
	C2	BMC	384	Philips
	C3	I2CVB	468	Siemens
	C4	UCL	175	Siemens
	C5	BIDMC	261	General Electric
	C6	HK	157	Siemens
Fed-COSAS (Pathology)	C1	teksqray-600p	60	TEKSQRAY SQS-600P
	C2	kfbio-400	60	KFBIO KF-PRO-400
	C3	3d-1000	60	3DHISTECH PANNORAMIC 1000
Fed-BUS (Ultrasound)	C1	BUID [46]	232	Supersonic Imagine Aixplorer Ultimate
	C2	BUSI [47]	630	N/A
	C3	BUS_UC [48]	811	N/A
	C4	BUS_UCLM [49]	264	Siemens ACUSON S2000TM Ultrasound System
Fed-MG (Infrared)	C1	MGD-1k [50]	1,000	LipiView II Ocular Surface Interferometer
	C2	CAMG [51]	100	Keratograph 5 M (Oculus, Germany)
Fed-Polyp (Endoscopic)	C1	CVC-300 [52]	60	N/A
	C2	CVC-ClinicDB [53]	612	Hospital Clinic of Barcelona, Spain / Colonoscopy
	C3	CVC-ColonDB [54]	380	Colonoscopy
	C4	EndoTect [55]	200	Endoscopy
	C5	ETISLarib-PolypDB [56]	196	Wireless Capsule Endoscopy

We provide a brief description of each dataset in the FL-MedSegBench benchmark suite, which is summarized in Tables I and II.

**Fed-Vessel.** This dataset is constructed for the task of retinal blood vessel segmentation with 2D fundus images, comprising six client data sources: chaseDB [40], DR-Hagis [41], DRIVE [42], HRF [43], LES-AV [44], and ORVS [45]. chaseDB contains 28 images captured with Nidek NM-200-D fundus cameras; DR-Hagis includes 40 images acquired using three different devices, *i.e.*, the Canon CR DGi, the Topcon TRC-NW6s, and the Topcon TRC-NW8; DRIVE consists of 40 images obtained with Canon CR5 nonmydriatic 3CCD cameras and TopCon TRV-50 fundus cameras; HRF contains 45 images captured by the Canon CF-60 UVi; LES-AV includes 22 images; ORVS comprises 49 images collected using the Zeiss Visucam 200. All clients provide predefined training and test splits. We further split their training sets into training and validation subsets with a ratio of 4:1. Images are resized to  $256 \times 256$ .

**Fed-Prostate.** This dataset [57] is constructed for the prostate segmentation task with 2D MRI slices, comprising six client data sources: RUNMC, BMC, I2CVB, UCL, BIDMC, and HK. RUNMC contains 411 images from 30 patients acquired with Siemens scanners; BMC includes 384 images from 30 patients obtained using Philips equipment; I2CVB consists of 468 images from 19 patients captured with Siemens devices; UCL contains 175 images from 13 patients from Siemens scanners; BIDMC includes 261 images from 12 patients

collected with General Electric systems; and HK comprises 157 images from 12 patients also acquired using Siemens scanners. We randomly split the patients of each client into training, validation, and test sets with a ratio of 7:1:2 and crop the center region of each image with the size  $256 \times 256$ .

**Fed-COSAS.** Fed-COSAS [58] is built for adenocarcinoma segmentation with 2D pathology slides. The dataset comprises image patches extracted from whole slide image scans of invasive breast carcinoma tissues, acquired with 3 different scanners (TEKSQRAY SQS-600P, KFBIO KF-PRO-400 and 3DHISTECH PANNORAMIC 1000). Each scanner produces 60 images. We randomly split the data of per client into training, validation, and test sets with a ratio of 7:1:2. All images are resized to  $256 \times 256$ .

**Fed-BUS.** This dataset is constructed for the task of breast tumor segmentation with 2D ultrasound images, comprising four client data sources: BUID [46], BUSI [47], BUS\_UC [48], and BUS\_UCLM [49]. BUID contains 232 images acquired using AirProrer Ultimate and Supersonic Imagine ultrasound machines; BUSI includes 630 images, for which the acquisition device is not specified; BUS\_UC consists of 811 images, also without device information provided; and BUS\_UCLM comprises 264 images captured with the Siemens ACUSON S2000TM Ultrasound System. The data of per client are splitted into training, validation, and test sets with a ratio of 7:1:2. All images are resized to  $256 \times 256$ .

**Fed-MG.** This dataset is constructed for the task of meibomian gland segmentation with 2D infrared images, comprising two

TABLE II: Summary of the 3D medical datasets in FL-MedSegBench

Dataset	Index	Client name	Sample size	Devices/Institutions
Fed-Pancreas (MRI-T1)	C1	NYU	162	New York University Medical Center
	C2	MCF	151	Mayo Clinic Florida
	C3	NU	30	Northwestern University
	C4	AHN	17	Allegheny Health Network
	C5	MCA	25	Mayo Clinic Arizona
Fed-M&Ms (CMR)	C1	Centre 1	95	Vall d’Hebron Hospital, Spain / Siemens
	C2	Centre 2	74	Sagrada Familia Clínica, Spain / Philips
	C3	Centre 3	51	Universitätsklinikum Hamburg-Eppendorf, Germany / Philips
	C4	Centre 4	50	Universitari Dexeus Hospital, Spain / General Electric
	C5	Centre 5	50	Creu Blanca Clínica, Spain / Canon
FeTS2022 (MRI-T1 / T1-Gd / MRI-T2 / T2-FLAIR)	C1	Centre 1	170	N/A
	C2	Centre 2	170	N/A
	C3	Centre 3	171	N/A
	C4	Centre 4	34	N/A
	C5	Centre 5	30	N/A
	C6	Centre 6	127	N/A
	C7	Centre 7	127	N/A
	C8	Centre 8	128	N/A
	C9	Centre 9	33	N/A

client data sources: MGD-1k [50] and CAMG [51]. MGD-1k contains 1,000 images acquired using the LipiView II Ocular Surface Interferometer, while CAMG consists of 100 images, for which specific acquisition device information is not specified. We randomly split the data of each client into training, validation, and test sets with a ratio of 7:1:2. Images are resized to  $192 \times 384$ .

**Fed-Polyp.** This dataset is constructed for polyp segmentation task with 2D endoscopic images, comprising five client data sources: CVC-300 [52] with 60 images, CVC-ClinicDB [53] with 612 images, CVC-ColonDB [54] with 380 images, EndoTect [55] with 200 images, and ETISLarib-PolypDB [56] with 196 images. Among these, both CVC-ClinicDB and CVC-ColonDB were captured using colonoscopes, while the specific acquisition devices for the remaining datasets are not explicitly provided. The data of each client are randomly divided into training/validation/test sets with a ratio of 7:1:2. Images are resized to  $256 \times 256$ .

**Fed-Pancreas.** This dataset [59] is constructed for the pancreas segmentation task with 3D MRI T1 volumes, comprising five client data sources: New York University (NYU) Medical Center with 162 scans, Mayo Clinic Florida (MCF) with 151 scans, Northwestern University (NU) with 30 scans, Allegheny Health Network (AHN) with 17 scans, and Mayo Clinic Arizona (MCA) with 25 scans. The specific medical imaging devices used for acquisition are not detailed for any of the contributing clients in this federated collection. We divide the data of each client into training/validation/test sets with a ratio of 7:1:2 and randomly sample patches with the size  $32 \times 256 \times 256$  as input of model.

**Fed-M&Ms.** This dataset [60] is built for right ventricular segmentation task with 3D MRI volumes, comprising 5 center data sources including four hospitals from Spain and one hospital from Germany. The Vall d’Hebron Hospital contains 95 volumes acquired using Siemens scanners; the Sagrada Familia Hospital includes 74 images obtained with Philips

systems; Universitätsklinikum Hamburg-Eppendorf provides 51 volumes from Philips scanners; Both Universitari Dexeus Hospital and Creu Blanca Clínica contain 50 volumes captured by General Electric and Canon imaging systems, respectively. We divide data of per client into training/validation/test sets with a ratio of 7:1:2 and randomly sample patches with the size  $16 \times 256 \times 256$  as input of model.

**FeTS2022.** This dataset is from the Federated Tumor Segmentation (FeTS) 2022 challenge [61], which mainly focuses on the construction and evaluation of a consensus model for the brain tumor segmentation task. The dataset contains 1251 patients from 33 institutions. The data of each patient is acquired by multi-parametric magnetic resonance imaging (mpMRI) and has four modalities: T1-Weighted MRI (MRI-T1), post-contrast T1-weighted MRI (MRI-T1Gd), T2-Weighted MRI (MRI-T2), and T2 Fluid Attenuated Inversion Recovery (T2-FLAIR). Besides normal regions, annotations comprise the GD-enhancing tumor (ET), the peritumoral edematous/invaded tissue (ED), and the necrotic tumor core (NCR). We selected the institutions with more than 30 patients, forming 9 clients. We divide the data of each client into training/validation/test sets with a ratio of 7:1:2 and center-crop per modality and obtain patches with size  $4 \times 128 \times 128 \times 128$  as input to the model.

## B. Methods

In FL-MedSegBench, we conduct extensive comparisons of various FL methods, encompassing eight gFL methods (FedAvg [9], FedProx [15], MOON [20], FedAWA [21], FedNova [22], FedRDN [25], PN [62] and FedLWS [23]) and five pFL methods (FedRoD [31], SiobN [33], FedBN [34], FedPer [30] and Ditto [32]).

**FedAvg.** FedAvg [9] serves as the simplest FL algorithm, operating through iterative rounds of local stochastic gradient descent updates on clients followed by a simple averaging of model parameters on a central server. FedAvg’s performance

TABLE III: The segmentation performance (Dice) of different methods on Fed-Vessel dataset (%).

Methods	C1	C2	C3	C4	C5	C6
Local	77.96 $\pm$ 0.76	70.43 $\pm$ 0.24	77.00 $\pm$ 0.55	74.75 $\pm$ 0.25	78.41 $\pm$ 0.55	71.34 $\pm$ 0.39
<i>Generic FL methods</i>						
FedAvg	74.97 $\pm$ 0.90	68.50 $\pm$ 0.32	70.43 $\pm$ 0.70	74.98 $\pm$ 0.27	78.13 $\pm$ 0.08	71.02 $\pm$ 0.19
FedAWA	77.12 $\pm$ 0.57	68.45 $\pm$ 0.65	72.45 $\pm$ 0.61	75.17 $\pm$ 0.31	79.17 $\pm$ 0.19	70.41 $\pm$ 0.33
FedLWS	<b>79.96</b> $\pm$ 0.37	<b>70.24</b> $\pm$ 0.32	<b>74.29</b> $\pm$ 0.67	<b>76.25</b> $\pm$ 0.16	<b>80.35</b> $\pm$ 0.21	70.61 $\pm$ 0.57
FedNova	77.23 $\pm$ 0.93	68.86 $\pm$ 0.25	72.65 $\pm$ 0.36	75.38 $\pm$ 0.38	79.34 $\pm$ 0.37	70.46 $\pm$ 0.11
FedProx	75.08 $\pm$ 1.64	68.56 $\pm$ 0.36	70.83 $\pm$ 0.20	75.05 $\pm$ 0.30	78.07 $\pm$ 0.41	70.87 $\pm$ 0.54
FedRDN	75.68 $\pm$ 0.74	67.81 $\pm$ 0.69	69.87 $\pm$ 0.47	75.24 $\pm$ 0.16	78.43 $\pm$ 0.50	<b>71.29</b> $\pm$ 0.18
MOON	75.48 $\pm$ 1.14	68.79 $\pm$ 0.47	70.76 $\pm$ 0.30	75.08 $\pm$ 0.38	78.59 $\pm$ 0.21	70.71 $\pm$ 0.38
PN	70.83 $\pm$ 2.10	57.94 $\pm$ 3.89	69.97 $\pm$ 1.09	67.76 $\pm$ 1.78	71.72 $\pm$ 1.94	65.96 $\pm$ 1.45
<i>Personalized FL methods</i>						
Ditto	66.22 $\pm$ 1.96	62.74 $\pm$ 0.54	71.71 $\pm$ 0.67	70.69 $\pm$ 0.38	55.79 $\pm$ 9.73	67.38 $\pm$ 0.26
FedBN	<b>79.67</b> $\pm$ 0.64	<b>69.62</b> $\pm$ 0.30	<b>76.99</b> $\pm$ 0.34	<b>75.44</b> $\pm$ 0.50	<b>80.39</b> $\pm$ 0.13	<b>72.20</b> $\pm$ 0.08
FedPer	77.89 $\pm$ 1.37	68.65 $\pm$ 0.31	74.84 $\pm$ 0.34	75.08 $\pm$ 0.33	79.56 $\pm$ 0.24	71.68 $\pm$ 0.26
FedRoD	40.64 $\pm$ 12.90	36.99 $\pm$ 25.09	56.85 $\pm$ 11.09	65.54 $\pm$ 6.07	53.83 $\pm$ 9.83	53.34 $\pm$ 9.96
SioBN	78.64 $\pm$ 0.82	69.08 $\pm$ 0.38	75.70 $\pm$ 0.50	74.92 $\pm$ 0.23	80.05 $\pm$ 0.17	72.09 $\pm$ 0.34

is known to degrade under significant data heterogeneity, especially with many local update steps [15].

**FedProx.** FedProx [15] modifies FedAvg by incorporating a proximal term into the local objective function, with the aim of improving stability under statistical heterogeneity. This term explicitly regularizes the distance between the local and global models, effectively mitigating client drift during local training.

**MOON.** MOON [20] addresses client data heterogeneity through model-level contrastive learning. It corrects local updates by maximizing the agreement between the representations learned by the current local model and those from the global model, based on the observation that the global model, trained on the entire dataset, generally learns more robust representations than local models trained on skewed data subsets.

**FedAWA.** FedAWA [21] uses an adaptive weighting mechanism during server aggregation by dynamically adjusting weights based on client vectors. These vectors capture the direction of local model updates, reflecting variations in client data distributions. This approach enhances robustness against non-IID data without requiring additional datasets or compromising privacy.

**FedNova.** FedNova [22] tackles the objective inconsistency caused by heterogeneous client participation and varying numbers of local updates. It proposes a normalized averaging scheme on server, which accounts for differences in local update progress to ensure convergence to a consistent stationary point while maintaining a fast convergence rate.

**FedRDN.** FedRDN [25] addresses the feature shift caused by non-IID data in FL through an input-level data augmentation method. It enhances the generalization of local feature representations by randomly injecting global statistical information into the client’s local data, thereby enhancing the generalization of local feature representations.

**PN.** PN [62] addresses the limitations of batch normalization in FL by learning the normalization statistics as trainable parameters, rather than computing them from client mini-batches. This creates homogeneous normalization layers across clients, stabilizing training under data heterogeneity and enabling effective learning even with very small batch sizes.

**FedLWS.** FedLWS [23] addresses the global weight shrinking effect in FL by adaptively designing layer-wise shrinking factors during model aggregation. It calculates these factors based on distinctions among different layers of the global model.

**FedRoD.** FedRoD [31] bridges the gap between generalization and personalization by decoupling learning into two components: a global predictor trained with a consistent objective across clients, and a lightweight client-specific module optimized on top of it to minimize each client’s empirical risk. This dual-predictor framework simultaneously achieves strong global performance and effective local adaptation in heterogeneous federated settings.

**SioBN.** SioBN [33] addresses multi-centric data heterogeneity in federated medical imaging by keeping batch normalization (BN) statistics local to each client (or silo), while only averaging the weight parameters globally. This approach maintains data privacy, adapts to site-specific characteristics, and reduces potential information leakage.

**FedBN.** FedBN [34] alleviates feature shift in non-IID settings by localizing BN layers. While convolutional layers are aggregated centrally, each client maintains its own batch-specific statistics. This allows the model to adapt to local data distributions without sharing normalization parameters.

**FedPer.** FedPer [30] introduces personalized FL by splitting the model into base and personalization layers. While the base layers are trained collaboratively using federated averaging, the personalization layers are updated locally on each device, effectively capturing user-specific characteristics while maintaining a shared feature representation.

**Ditto.** Ditto [32] jointly learns a global model and personalized local models through a multi-task learning objective. It introduces a regularization term that penalizes the deviation of each personalized model from the global model, allowing a tunable balance between local adaptation and global consensus.

### C. Implementation details

We implement FL-MedSegBench based on the PyTorch platform. We use the Adam optimizer [63] for all datasets. The initial learning rate is selected from  $\{0.01, 0.001, 0.0001\}$

TABLE IV: The segmentation performance (Dice) of different methods on Fed-Prostate dataset (%).

Methods	C1	C2	C3	C4	C5	C6
Local	76.37 ± 2.19	86.41 ± 1.94	80.30 ± 1.64	84.06 ± 2.56	86.74 ± 0.76	62.32 ± 3.33
<i>Generic FL methods</i>						
FedAvg	<b>76.35</b> ± 2.39	86.29 ± 0.84	87.06 ± 0.36	87.15 ± 2.31	88.99 ± 1.22	78.48 ± 3.51
FedAWA	74.84 ± 7.54	86.99 ± 0.59	87.83 ± 1.30	86.47 ± 0.48	89.11 ± 0.54	78.84 ± 3.47
FedLWS	74.49 ± 3.96	<b>88.33</b> ± 0.28	<b>89.17</b> ± 0.70	87.71 ± 1.53	<b>89.37</b> ± 0.71	<b>80.45</b> ± 1.66
FedNova	74.94 ± 8.94	86.45 ± 0.32	87.99 ± 0.82	<b>88.22</b> ± 0.97	88.67 ± 0.24	78.03 ± 3.20
FedProx	76.00 ± 2.99	86.56 ± 0.80	87.86 ± 0.58	87.20 ± 1.70	89.33 ± 0.50	77.00 ± 2.60
FedRDN	71.92 ± 8.24	86.84 ± 0.34	86.15 ± 1.29	88.12 ± 2.18	88.94 ± 0.24	78.58 ± 2.75
MOON	75.26 ± 3.72	86.66 ± 0.26	86.87 ± 0.40	87.58 ± 1.76	88.63 ± 0.11	77.67 ± 3.52
PN	75.24 ± 6.26	86.39 ± 1.25	87.00 ± 0.53	86.55 ± 1.66	88.96 ± 0.84	77.25 ± 4.72
<i>Personalized FL methods</i>						
Ditto	<b>78.42</b> ± 0.48	84.11 ± 0.62	83.43 ± 1.48	84.61 ± 2.84	84.88 ± 0.98	<b>77.83</b> ± 2.66
FedBN	73.86 ± 6.40	<b>88.31</b> ± 0.49	<b>87.68</b> ± 0.60	87.95 ± 1.95	88.07 ± 0.25	75.44 ± 3.65
FedPer	76.64 ± 1.21	86.48 ± 0.81	86.01 ± 1.28	<b>88.13</b> ± 0.47	<b>89.12</b> ± 0.37	75.96 ± 3.31
FedRoD	71.02 ± 3.44	83.98 ± 0.96	85.97 ± 0.61	87.98 ± 1.92	86.62 ± 2.00	62.38 ± 26.17
SioBN	78.07 ± 4.36	88.19 ± 0.62	83.24 ± 5.24	87.11 ± 3.34	88.32 ± 0.48	76.03 ± 6.49

via grid search. Two learning rate scheduling strategies are considered: keeping the learning rate constant or halving it every  $E/4$  rounds, where  $E$  denotes the total number of training rounds. In our experiments, for Fed-Vessel and Fed-MG, we set the initial learning rate to 0.001 and apply the halving schedule every  $E/4$  rounds. For the remaining datasets, a fixed learning rate of 0.0001 is used. The batch size is set to 8 for Fed-Vessel, Fed-Prostate, Fed-Polyp, and Fed-BUS; 4 for Fed-MG, Fed-COSAS, and FeTS2022; and 2 for Fed-Pancreas and Fed-M&Ms. We set  $\mu$  to 0.001 in FedProx and Ditto, 0.01 in MOON as suggested in their official implementations. We adopt the 2D U-Net [64] as the backbone network of all 2D datasets and 3D U-Net for Fed-M&Ms and FeTS2022. SA-Net [65] is used for Fed-Pancreas. During training, we apply data augmentation including Gaussian noise, elastic deformation, brightness and contrast adjustments, random horizontal and vertical flips, random 90-degree rotations, and random cropping. Performance is measured by Dice coefficient, and all results are averaged over three independent trials with mean and standard deviation reported. To show degrees of fairness of different FL methods, we report the equally-weighted average of Dice scores (aDice), the worst-client Dice scores (wDice), and the standard deviation (Std) of Dice scores of clients.

#### IV. EXPERIMENTAL RESULTS AND ANALYSIS

##### A. Performance Analysis

In this section, we compare the segmentation performance of various gFL and pFL methods across different medical tasks. The number of communication rounds  $T$  is set to 100 for all datasets.

1) *Performance Analysis of gFL Methods: Fed-Vessel.* Among gFL methods, FedLWS demonstrates superior performance, achieving the highest scores in five out of six clients (C1 to C5) within its category, as shown in Table III. Its performance on C1 (79.96%) and C5 (80.35%) surpasses the local baseline training, suggesting its adaptive weighting mechanism is particularly effective at leveraging cross-client information without succumbing to client drift. In contrast, standard methods like FedAvg and FedProx show a noticeable performance degradation compared with local training

on several clients (*e.g.*, FedAvg on C3 drops to 70.43% from 77.00%), a classic sign of model divergence under data heterogeneity. Methods like FedAWA, FedNova, and MOON offer marginal improvements over vanilla FedAvg on some clients but fail to consistently outperform the local training across all clients. PN exhibits the weakest performance overall, with high variance and significantly lower scores (*e.g.*, 57.94% on C2), indicating its instability in this federated context.

**Fed-Prostate.** According to Table IV, FedLWS emerges as the most robust and high-performing method. It achieves the best overall scores on four out of six clients, with particularly notable results on C3 (89.17%) and C5 (89.37%), surpassing all competitors by a clear margin. This reinforces the effectiveness of its adaptively layer-wise aggregation strategy. FedNova also demonstrates strong performance, securing the top position on C4 (88.22%). Standard methods like FedAvg and FedProx perform competitively on several clients, often matching or slightly exceeding the local training, but they do not achieve the peak performance of FedLWS. For instance, on C3, FedAvg reaches 87.06%, which is strong but still 2.11 percentage points behind FedLWS. Methods like FedAWA, FedRDN, MOON, and PN show comparable performance on most clients but exhibit higher variance on C1 (*e.g.*, FedRDN: 71.92%), suggesting that these methods may be less stable when learning from the specific data characteristics of this client, potentially due to its unique acquisition protocol or patient population.

**Fed-COSAS.** From Table V(a), FedRDN and PN emerge as the top performers. FedRDN achieves the highest score on C1 (77.67%) and a near-best result on C3 (79.83%). PN, on the other hand, secures the best overall performance on C2 (67.79%) and C3 (80.40%), outperforming all competitors on these clients. In contrast, standard methods like FedAvg and FedProx consistently underperform relative to the local training on C1 and C2 (*e.g.*, FedAvg: 68.53% on C1 vs. Local 71.99%), indicating that simple averaging suffers from client drift under severe domain shifts. FedLWS, despite its success on previous datasets, shows degraded performance here (*e.g.*, 57.11% on C2), suggesting that its loss-based weighting may be sensitive to the specific heterogeneity patterns of Fed-

TABLE V: The segmentation performance (Dice) of FL methods on Fed-COSAS and Fed-BUS datasets (%).

(a): Fed-COSAS				(b): Fed-BUS				
Methods	C1	C2	C3	Methods	C1	C2	C3	C4
Local	71.99 ± 7.65	68.21 ± 3.04	74.15 ± 9.04	Local	82.72 ± 0.19	74.58 ± 1.96	90.30 ± 0.08	74.86 ± 0.91
<i>Generic FL methods</i>				<i>Generic FL methods</i>				
FedAvg	68.53 ± 9.44	60.14 ± 5.83	71.61 ± 2.63	FedAvg	86.32 ± 1.07	73.72 ± 1.06	90.56 ± 0.55	71.90 ± 2.73
FedAWA	69.68 ± 9.19	61.82 ± 3.23	70.68 ± 2.93	FedAWA	85.69 ± 0.40	<b>74.89</b> ± 1.49	89.56 ± 0.46	77.11 ± 3.05
FedLWS	68.54 ± 8.77	57.11 ± 8.56	72.07 ± 3.71	FedLWS	84.63 ± 0.35	70.11 ± 0.63	87.90 ± 0.23	68.59 ± 4.94
FedNova	68.53 ± 9.44	60.14 ± 5.83	71.61 ± 2.63	FedNova	<b>86.35</b> ± 1.14	73.44 ± 1.67	89.55 ± 0.38	<b>77.30</b> ± 4.06
FedProx	69.10 ± 8.45	59.25 ± 6.37	70.52 ± 2.12	FedProx	85.68 ± 1.99	74.39 ± 1.83	90.04 ± 0.58	72.52 ± 4.16
FedRDN	<b>77.67</b> ± 4.50	67.60 ± 3.19	79.83 ± 0.15	FedRDN	86.30 ± 0.74	73.33 ± 1.00	<b>90.78</b> ± 0.57	71.34 ± 5.33
MOON	67.30 ± 10.06	61.29 ± 7.33	72.35 ± 4.38	MOON	85.77 ± 1.35	73.88 ± 1.89	90.09 ± 0.16	74.57 ± 1.35
PN	73.96 ± 3.70	<b>67.79</b> ± 4.21	<b>80.40</b> ± 1.91	PN	85.99 ± 1.45	73.04 ± 2.04	90.56 ± 0.53	73.63 ± 1.53
<i>Personalized FL methods</i>				<i>Personalized FL methods</i>				
Ditto	72.02 ± 5.56	64.64 ± 4.23	71.01 ± 1.96	Ditto	82.30 ± 0.91	74.46 ± 0.33	88.53 ± 0.78	71.64 ± 0.93
FedBN	<b>76.32</b> ± 4.69	<b>67.64</b> ± 3.06	<b>79.21</b> ± 1.21	FedBN	85.45 ± 2.66	<b>74.52</b> ± 0.95	<b>91.04</b> ± 0.19	70.62 ± 4.60
FedPer	71.59 ± 7.70	58.24 ± 4.35	71.43 ± 2.88	FedPer	<b>86.44</b> ± 0.62	73.77 ± 1.62	90.68 ± 0.93	<b>73.36</b> ± 3.14
FedRoD	54.64 ± 22.90	50.61 ± 7.26	69.20 ± 4.36	FedRoD	81.86 ± 2.32	73.03 ± 2.21	89.89 ± 1.26	73.28 ± 1.38
SioBN	75.92 ± 5.17	67.34 ± 2.58	78.41 ± 2.88	SioBN	85.00 ± 1.06	73.49 ± 0.55	90.62 ± 0.42	71.71 ± 1.47

COSAS.

**Fed-BUS.** As shown in Table V(b), FedNova and FedRDN demonstrate the consistent performance. FedNova achieves the highest score on C1 (86.35%) and ties for the best on C4 (77.30%), showcasing the benefit of its normalized gradient aggregation. FedRDN secures the top position on C3 (90.78%) and performs competitively on other clients. FedAWA also stands out, achieving the best result on C2 (74.89%) and strong performance on C4 (77.11%), indicating its adaptive weighting mechanism effectively handles client heterogeneity. Notably, FedLWS, which excelled on previous datasets, shows degraded performance here, particularly on C2 (70.11%) and C4 (68.59%), suggesting that its loss-based weighting strategy may be less suited to the specific domain characteristics of ultrasound imaging. Standard methods like FedAvg and FedProx perform reasonably well on C1 and C3 but struggle on the more challenging C4, where they fall short of the local training.

**Fed-MG.** As demonstrated in Table VI(a), FedAvg achieves the highest performance on C1 (79.07%), though this remains below the local training. FedNova secures the top generic result on C2 (69.86%), demonstrating the benefit of its normalized aggregation scheme. Methods such as FedAWA, FedProx, and MOON perform comparably, hovering around 78~79% on C1 and 69% on C2, but none successfully bridge the gap to local training. FedLWS and PN exhibit noticeable performance degradation, particularly on C2 where PN drops to 65.39%, suggesting that their respective weighting and proximal mechanisms may over-regularize in this two-client setting. This underperformance relative to the local training underscores the difficulty of extracting beneficial shared representations when only two heterogeneous clients participate.

**Fed-Polyp.** As shown in Table VI(b), FedNova achieves the highest score on C1 (91.00%) and remains competitive on other clients. FedRDN delivers the most consistent performance across clients: it secures the top generic result on C2 (86.78%) and C3 (78.69%), and achieves the highest Dice on C5 (65.85%) among generic methods—a critical advantage on this challenging client. FedLWS stands out on C4, reaching 80.06%, the highest among all methods. FedAvg,

FedAWA, FedProx, and MOON perform well on C1–C3 but suffer catastrophic degradation on C5 (e.g., FedAvg: 49.68%), highlighting the vulnerability of standard aggregation to outlier clients.

**Fed-Pancreas.** In Table VII, the local training exhibits severe performance degradation on clients with limited data (e.g., 22.58% on C1 and 16.23% on C3), underscoring the necessity of collaborative FL to improve generalization. Among generic FL methods, FedRDN achieves the highest performance, securing the best results on three clients (C2: 74.37%, C4: 73.88%, C5: 74.99%) and competitive scores on the remaining ones. FedProx excels on C1 (61.23%), while FedNova obtains the top score on C3 (41.83%). These results suggest that different aggregation or regularization strategies cater to different types of client heterogeneity. Notably, FedRDN’s consistent superiority may be attributed to its robustness in handling domain shifts.

**Fed-M&Ms.** As shown in Table VIII, on the M&Ms dataset, all generic FL methods except PN maintain relatively high performance across the five clients, without clear performance separation. FedRDN achieves the highest result on C1 with 82.33%, FedAWA reaches 85.66% on C2, FedAvg attains the best performance on C3 with 87.85%, and FedNova performs best on C4 with 81.78%. On C5, FedAWA achieves the highest score of 79.76%. Overall, different methods show client-specific advantages, and no single approach consistently dominates across all clients. In contrast, PN yields substantially lower performance on all clients, indicating a noticeable performance gap.

**FeTS2022.** Table IX presents the experimental results on the FeTS2022 dataset. FedProx, FedRDN, and FedNova demonstrate robust performance across clients. FedProx achieves the highest generic scores on C1 (78.63%), C2 (88.83%), and C7 (86.01%), showcasing the effectiveness of its proximal term in stabilizing training under heterogeneity. FedRDN secures the top generic results on C3 (88.77%), C6 (80.54%), and C8 (90.64%). FedNova leads on C4 (83.17%) and C9 (88.79%), benefiting from its normalized gradient aggregation. FedAvg and FedAWA also perform competitively, often ranking among the top two or three on multiple clients. In contrast, MOON

TABLE VI: The segmentation performance (Dice) of FL methods on Fed-MG and Fed-Polyp datasets (%).

(a): Fed-MG			(b): Fed-Polyp					
Methods	C1	C2	Methods	C1	C2	C3	C4	C5
Local	80.94 ± 1.55	71.28 ± 2.54	Local	72.84 ± 6.79	88.33 ± 0.82	80.03 ± 2.23	65.41 ± 4.76	71.59 ± 0.58
<i>Generic FL methods</i>			<i>Generic FL methods</i>					
FedAvg	<b>79.07</b> ± 1.71	69.60 ± 3.51	FedAvg	89.99 ± 1.55	85.14 ± 2.80	78.06 ± 2.34	68.94 ± 2.71	49.68 ± 4.95
FedAWA	78.55 ± 1.56	69.79 ± 3.58	FedAWA	90.83 ± 1.77	80.70 ± 3.70	76.42 ± 2.35	70.98 ± 4.01	53.55 ± 1.86
FedLWS	77.11 ± 0.91	66.52 ± 2.60	FedLWS	87.38 ± 6.74	81.14 ± 4.16	69.98 ± 4.12	<b>80.06</b> ± 3.84	49.38 ± 9.92
FedNova	77.37 ± 1.37	<b>69.86</b> ± 3.54	FedNova	<b>91.00</b> ± 2.09	80.57 ± 3.15	77.46 ± 3.07	71.79 ± 7.47	58.79 ± 5.15
FedProx	78.95 ± 2.23	69.21 ± 3.42	FedProx	90.46 ± 1.58	83.92 ± 2.38	76.40 ± 2.50	70.52 ± 2.42	47.57 ± 7.24
FedRDN	78.65 ± 1.19	69.48 ± 3.67	FedRDN	90.29 ± 2.10	<b>86.78</b> ± 2.32	<b>78.69</b> ± 3.72	72.64 ± 5.53	<b>65.85</b> ± 0.60
MOON	78.90 ± 1.53	69.58 ± 3.98	MOON	90.37 ± 0.81	84.63 ± 2.78	78.24 ± 1.91	68.99 ± 4.03	50.71 ± 7.39
PN	77.35 ± 1.09	65.39 ± 4.39	PN	88.45 ± 2.01	85.84 ± 2.57	77.01 ± 1.74	77.53 ± 3.09	52.99 ± 8.01
<i>Personalized FL methods</i>			<i>Personalized FL methods</i>					
Ditto	78.78 ± 0.50	68.24 ± 2.42	Ditto	77.32 ± 4.85	84.78 ± 1.70	75.12 ± 2.42	71.85 ± 4.62	<b>68.07</b> ± 5.10
FedBN	<b>79.46</b> ± 1.91	<b>70.54</b> ± 4.19	FedBN	85.87 ± 4.56	<b>87.72</b> ± 1.06	<b>79.48</b> ± 1.53	<b>78.27</b> ± 3.96	60.19 ± 4.49
FedPer	78.09 ± 0.88	68.74 ± 2.66	FedPer	<b>89.46</b> ± 2.55	84.35 ± 1.82	77.46 ± 2.77	68.81 ± 4.04	49.52 ± 6.92
FedRoD	65.48 ± 20.53	69.48 ± 3.48	FedRoD	88.92 ± 1.18	83.46 ± 1.16	76.31 ± 4.19	69.44 ± 4.63	33.98 ± 7.05
SioBN	79.18 ± 1.08	64.12 ± 1.19	SioBN	88.64 ± 2.07	87.05 ± 1.54	77.43 ± 1.38	74.67 ± 5.77	62.76 ± 1.73

TABLE VII: The performance (Dice) of different methods on Fed-Pancreas dataset.

Methods	C1	C2	C3	C4	C5
Local	22.58±11.84	68.14±1.78	16.23±8.95	58.57±5.38	72.00±2.24
<i>Generic FL methods</i>					
FedAvg	54.71±19.44	72.11±1.52	33.97±6.16	71.35±0.30	72.81±5.03
FedAWA	55.73±17.01	71.77±1.67	36.68±7.00	71.99±1.39	70.97±4.43
FedLWS	51.26±12.99	68.76±1.21	26.44±6.15	70.33±4.08	67.24±4.48
FedNova	53.40±15.76	72.93±1.67	<b>41.83</b> ±15.96	71.99±2.44	72.61±4.94
FedProx	<b>61.23</b> ±15.43	74.26±0.58	34.43±7.99	73.04±3.27	74.02±3.47
FedRDN	59.94±18.49	<b>74.37</b> ±1.01	32.99±9.82	<b>73.88</b> ±5.06	<b>74.99</b> ±3.39
MOON	55.67±13.96	72.33±3.79	33.37±6.54	72.00±5.75	72.95±4.06
PN	19.56±6.60	48.20±4.49	9.52±2.25	38.44±10.33	41.90±1.63
<i>Personalized FL methods</i>					
Ditto	17.84±13.32	67.50±2.10	14.60±7.67	57.18±3.10	72.50±4.29
FedBN	51.00±8.72	74.21±2.34	<b>34.36</b> ±8.88	70.95±1.64	<b>74.42</b> ±5.00
FedPer	56.96±9.63	73.13±1.56	33.60±5.77	73.54±1.99	74.33±2.92
FedRoD	<b>57.54</b> ±13.93	73.20±0.29	31.48±6.81	<b>73.58</b> ±5.01	73.90±4.32
SioBN	54.81±15.76	<b>74.24</b> ±0.37	33.89±6.54	73.05±5.03	73.20±3.43

and PN exhibit consistent underperformance: MOON lags behind on most clients (e.g., C4: 76.18% vs. best 83.17%), while PN collapses catastrophically, with scores dropping to 66~78%, far below even the local training. This reinforces the unsuitability of contrastive or proximal regularization for dense tasks.

2) *Performance Analysis of pFL Methods: Fed-Vessel.* In Table III, FedBN emerges as the top-performing method across all clients (C1 to C6). Its performance on C3 (76.99%), C5 (80.39%), and C6 (72.20%) not only surpasses all generic FL methods but also consistently exceeds the local training. The results validate the core premise of FedBN: learning private batch normalization statistics for each client effectively captures domain-specific characteristics. SioBN and FedPer also demonstrate strong personalization capabilities, ranking as the second and third best. SioBN, for instance, achieves competitive results on C1 (78.64%) and C6 (72.09%), further emphasizing the importance of personalized feature normalization layers. Conversely, Ditto and FedRoD exhibit unstable and often poor performance.

**Fed-Prostate.** In Table IV, Ditto stands out on C1, achieving the highest score overall (78.42%), significantly outperforming

TABLE VIII: The performance (Dice) of different methods on Fed-M&Ms dataset.

Methods	C1	C2	C3	C4	C5
Local	81.18±1.90	82.32±2.27	82.85±1.25	72.00±1.33	76.70±3.06
<i>Generic FL methods</i>					
FedAvg	80.67±0.91	85.35±0.86	<b>87.85</b> ±0.76	79.28±1.60	79.00±0.63
FedAWA	78.75±1.83	<b>85.66</b> ±1.08	87.52±0.75	79.57±3.97	<b>79.76</b> ±1.41
FedLWS	79.52±0.83	85.32±0.51	87.52±0.66	79.71±0.81	79.55±2.79
FedNova	79.10±1.30	85.39±0.65	87.44±0.96	<b>81.78</b> ±1.16	79.01±1.40
FedProx	79.30±2.43	85.60±1.07	87.75±0.35	80.32±1.08	79.53±2.07
FedRDN	<b>82.33</b> ±0.33	85.56±0.84	87.05±1.04	80.85±1.16	76.92±1.50
MOON	79.21±1.63	85.54±1.01	87.29±0.73	80.80±0.80	78.40±2.40
PN	56.77±3.73	63.72±2.77	68.26±1.85	57.21±3.69	54.37±5.64
<i>Personalized FL methods</i>					
Ditto	81.44±0.80	82.39±1.36	79.42±2.87	75.85±1.71	74.75±4.61
FedBN	<b>82.84</b> ±0.51	85.57±1.07	<b>87.39</b> ±0.67	80.93±0.31	78.81±0.79
FedPer	80.15±1.41	85.54±0.82	87.31±0.84	80.83±0.98	<b>80.40</b> ±1.13
FedRoD	78.09±1.59	84.34±1.18	87.05±0.38	80.35±0.69	78.00±1.74
SioBN	82.52±0.61	<b>85.67</b> ±0.90	87.17±0.23	<b>81.29</b> ±0.74	75.77±2.62

both generic and other personalized methods on that client. This suggests that learning a personalized model while preserving a global objective is particularly beneficial for C1’s data characteristics. FedBN and FedPer also deliver strong results, with FedBN achieving strong results on C2 (88.31%) and C3 (87.68%), and FedPer achieving top performance on C4 (88.13%) and C5 (89.12%). This further validates the importance of personalized feature normalization and personalized layers in handling domain shifts. However, SioBN shows high variance on some clients (e.g., C3: 83.24 ± 5.24, C6: 76.03 ± 6.49), indicating potential instability. FedRoD exhibits catastrophic failure on C6 (62.38%), with extreme variance that renders its results unreliable, again underscoring its unsuitability for dense prediction tasks.

**Fed-COSAS.** From Table V(a), FedBN achieves strong results across all clients: 76.32% on C1, 67.64% on C2, and 79.21% on C3, ranking second on C1 and C3 and first on C2. SioBN follows closely with 75.92%, 67.34%, and 78.41% on C1~C3, respectively, reaffirming the benefit of client-specific batch normalization statistics. These pFL methods not only surpass the local training but also rival the best generic methods—FedBN’s performance on C1 and C3 is comparable to Fe-

TABLE IX: The segmentation performance (Dice) of different methods on FeTS2022 dataset (%).

Methods	C1	C2	C3	C4	C5	C6	C7	C8	C9
Local	78.01 $\pm$ 1.80	87.60 $\pm$ 1.57	88.06 $\pm$ 1.37	77.01 $\pm$ 2.55	82.45 $\pm$ 0.45	76.55 $\pm$ 2.88	85.80 $\pm$ 1.31	90.14 $\pm$ 1.22	79.63 $\pm$ 5.53
<i>Generic FL methods</i>									
FedAvg	78.40 $\pm$ 2.86	88.19 $\pm$ 2.13	87.90 $\pm$ 1.35	82.43 $\pm$ 5.70	<b>88.97</b> $\pm$ 3.17	79.77 $\pm$ 1.57	85.86 $\pm$ 1.55	90.25 $\pm$ 1.26	88.58 $\pm$ 2.37
FedAWA	77.60 $\pm$ 2.26	88.21 $\pm$ 1.06	87.53 $\pm$ 0.90	83.04 $\pm$ 5.08	88.32 $\pm$ 2.70	79.71 $\pm$ 1.44	85.02 $\pm$ 1.55	90.43 $\pm$ 0.60	88.62 $\pm$ 2.62
FedLWS	77.68 $\pm$ 3.07	88.38 $\pm$ 1.22	87.29 $\pm$ 1.10	82.48 $\pm$ 5.30	88.92 $\pm$ 2.86	80.15 $\pm$ 0.98	85.44 $\pm$ 1.65	89.76 $\pm$ 1.33	88.55 $\pm$ 2.28
FedNova	78.11 $\pm$ 1.85	88.33 $\pm$ 1.03	88.06 $\pm$ 0.87	<b>83.17</b> $\pm$ 4.75	88.90 $\pm$ 2.91	79.83 $\pm$ 1.15	85.39 $\pm$ 1.95	90.29 $\pm$ 0.48	<b>88.79</b> $\pm$ 2.22
FedProx	<b>78.63</b> $\pm$ 2.62	<b>88.83</b> $\pm$ 1.29	87.84 $\pm$ 1.09	81.80 $\pm$ 5.21	88.27 $\pm$ 3.58	79.47 $\pm$ 1.94	<b>86.01</b> $\pm$ 1.74	90.58 $\pm$ 0.63	88.66 $\pm$ 2.56
FedRDN	77.71 $\pm$ 3.74	88.23 $\pm$ 1.16	<b>88.77</b> $\pm$ 1.42	81.85 $\pm$ 6.00	88.93 $\pm$ 3.43	<b>80.54</b> $\pm$ 0.41	85.63 $\pm$ 1.82	<b>90.64</b> $\pm$ 0.90	88.62 $\pm$ 2.68
MOON	73.07 $\pm$ 4.94	83.69 $\pm$ 5.43	83.29 $\pm$ 3.85	76.18 $\pm$ 10.29	84.85 $\pm$ 4.17	75.90 $\pm$ 2.76	80.73 $\pm$ 6.09	85.53 $\pm$ 3.53	84.32 $\pm$ 2.40
PN	66.00 $\pm$ 1.40	77.14 $\pm$ 1.30	77.30 $\pm$ 1.70	68.46 $\pm$ 4.45	76.92 $\pm$ 3.45	67.02 $\pm$ 1.00	73.67 $\pm$ 2.87	78.73 $\pm$ 1.34	77.84 $\pm$ 2.20
<i>Personalized FL methods</i>									
Ditto	76.92 $\pm$ 2.16	87.79 $\pm$ 1.04	<b>88.19</b> $\pm$ 1.48	75.95 $\pm$ 1.52	78.95 $\pm$ 1.44	76.44 $\pm$ 1.58	83.38 $\pm$ 0.93	89.55 $\pm$ 1.07	82.34 $\pm$ 0.83
FedBN	<b>77.71</b> $\pm$ 2.32	<b>88.78</b> $\pm$ 1.00	88.14 $\pm$ 0.53	<b>82.98</b> $\pm$ 4.76	<b>89.22</b> $\pm$ 2.60	<b>80.74</b> $\pm$ 1.47	86.12 $\pm$ 1.49	89.82 $\pm$ 1.39	87.16 $\pm$ 3.40
FedPer	77.18 $\pm$ 2.27	88.52 $\pm$ 0.74	87.90 $\pm$ 1.01	80.82 $\pm$ 4.50	87.16 $\pm$ 3.05	79.65 $\pm$ 0.95	86.02 $\pm$ 1.32	<b>90.98</b> $\pm$ 0.97	86.92 $\pm$ 1.65
FedRoD	76.36 $\pm$ 1.59	87.79 $\pm$ 0.40	83.86 $\pm$ 5.03	80.28 $\pm$ 3.08	87.70 $\pm$ 1.77	79.70 $\pm$ 1.03	84.64 $\pm$ 2.77	89.86 $\pm$ 1.14	81.20 $\pm$ 9.04
SioBN	75.79 $\pm$ 1.64	87.86 $\pm$ 1.00	87.10 $\pm$ 1.39	81.46 $\pm$ 4.58	89.13 $\pm$ 2.79	78.95 $\pm$ 1.24	<b>86.19</b> $\pm$ 1.27	87.85 $\pm$ 1.24	<b>88.56</b> $\pm$ 2.23

TABLE X: The generalization performance (Dice) of different methods (%).

Methods	ARIA	IOSTAR	MSD	Kvasir-SEG	BUS
FedAvg	63.37 $\pm$ 0.85	63.96 $\pm$ 0.31	82.20 $\pm$ 1.36	72.11 $\pm$ 0.75	74.43 $\pm$ 0.74
FedAWA	64.79 $\pm$ 0.60	65.27 $\pm$ 0.79	82.13 $\pm$ 1.01	71.45 $\pm$ 0.71	<b>74.54</b> $\pm$ 1.32
FedLWS	<b>66.41</b> $\pm$ 0.58	<b>72.40</b> $\pm$ 2.21	<b>84.27</b> $\pm$ 1.36	20.69 $\pm$ 9.68	74.20 $\pm$ 0.37
FedNova	65.13 $\pm$ 0.61	65.79 $\pm$ 0.45	82.55 $\pm$ 0.72	73.43 $\pm$ 0.85	73.97 $\pm$ 2.41
FedProx	63.63 $\pm$ 0.62	63.74 $\pm$ 0.24	82.25 $\pm$ 1.42	72.99 $\pm$ 0.34	73.86 $\pm$ 1.38
MOON	62.94 $\pm$ 0.71	63.87 $\pm$ 0.86	82.18 $\pm$ 0.89	72.40 $\pm$ 0.56	73.52 $\pm$ 0.35
PN	60.71 $\pm$ 1.86	59.51 $\pm$ 1.93	83.72 $\pm$ 1.13	<b>74.17</b> $\pm$ 1.26	74.15 $\pm$ 3.50

drDN’s, while it ties with PN on C2. Ditto and FedPer show moderate improvements but do not consistently outperform the generic top performers. FedRoD also exhibits catastrophic failure on this dataset, with extremely low means and high variances.

**Fed-BUS.** In Table V(b), FedPer emerges as the top overall performer, achieving the highest score on C1 (86.44%) and C4 (73.36%). This underscores the value of maintaining client-specific feature extractors when domain shifts are pronounced. FedBN delivers the best performance on C3 (91.04%) and remains competitive on C2 (74.52%), reaffirming the importance of personalized batch normalization statistics. SioBN also performs strongly, particularly on C3 (90.62%) and C1 (85.00%). In contrast, Ditto and FedRoD consistently underperform both generic top performers and other personalized methods, with FedRoD showing particular weakness on C1 (81.86%).

**Fed-MG.** Table VI(a) reports the performance of pFL methods on Fed-MG. We observe that FedBN emerges as the overall best performer, achieving the highest scores on both C1 (79.46%) and C2 (70.54%). Critically, FedBN’s result on C2 surpasses all generic methods. SioBN also performs strongly on C1 (79.18%), though it shows unexpected weakness on C2 (64.12%), indicating potential instability in its normalization strategy for certain domains. Ditto and FedPer deliver moderate improvements but do not match FedBN’s performance. FedRoD exhibits catastrophic failure on C1 (65.48%), further confirming its unsuitability for segmentation tasks.

**Fed-Polyp.** As shown in Table VI(b), pFL methods exhibit noticeable performance variation across clients. FedBN achieves 87.72%, 79.48%, and 78.27% on C2, C3, and C4, respectively, demonstrating strong competitiveness. Ditto achieves

the highest score on C5 (68.07%), which is the only method to approach the local training, underscoring its effectiveness in learning personalized models while maintaining global structure. FedPer and SioBN also perform competitively on several clients, with SioBN achieving 87.05% on C2 and 88.64% on C1. FedRoD exhibits instability again, particularly on C5 (33.98%).

**Fed-Pancreas.** In Table VII, pFL methods still exhibit noticeable performance variation across clients on Fed-Pancreas. FedRoD achieves the highest result on C1 with 57.54%, while FedBN reaches 34.36% on C3 and 74.42% on C5, demonstrating certain competitiveness. SioBN attains 74.24% on C2, which is close to the best-performing generic method. In contrast, Ditto yields lower results on C1 and C3 with substantial fluctuations. FedPer maintains relatively stable performance across multiple clients but does not demonstrate a clear leading advantage.

**Fed-M&Ms.** As shown in Table VIII, FedBN achieves the highest overall score on C1 (82.84%) and ties for best on C2 (85.57%) and C3 (87.39%), reaffirming the value of client-specific batch normalization statistics. SioBN matches FedBN on C2 (85.67%) and secures the second-best result on C4 (81.29%), demonstrating its effectiveness. FedPer delivers the top score on C5 (80.40%), underscoring the benefit of personalized feature extractors. However, Ditto and FedRoD show weaker performance, particularly on C4 and C5, where they fall behind both generic leaders and other personalized methods. This suggests that their personalization mechanisms may not fully exploit the available cross-client knowledge.

**FeTS2022.** In Table IX, FedBN stands out as the most consistent pFL method, achieving top performance on C5

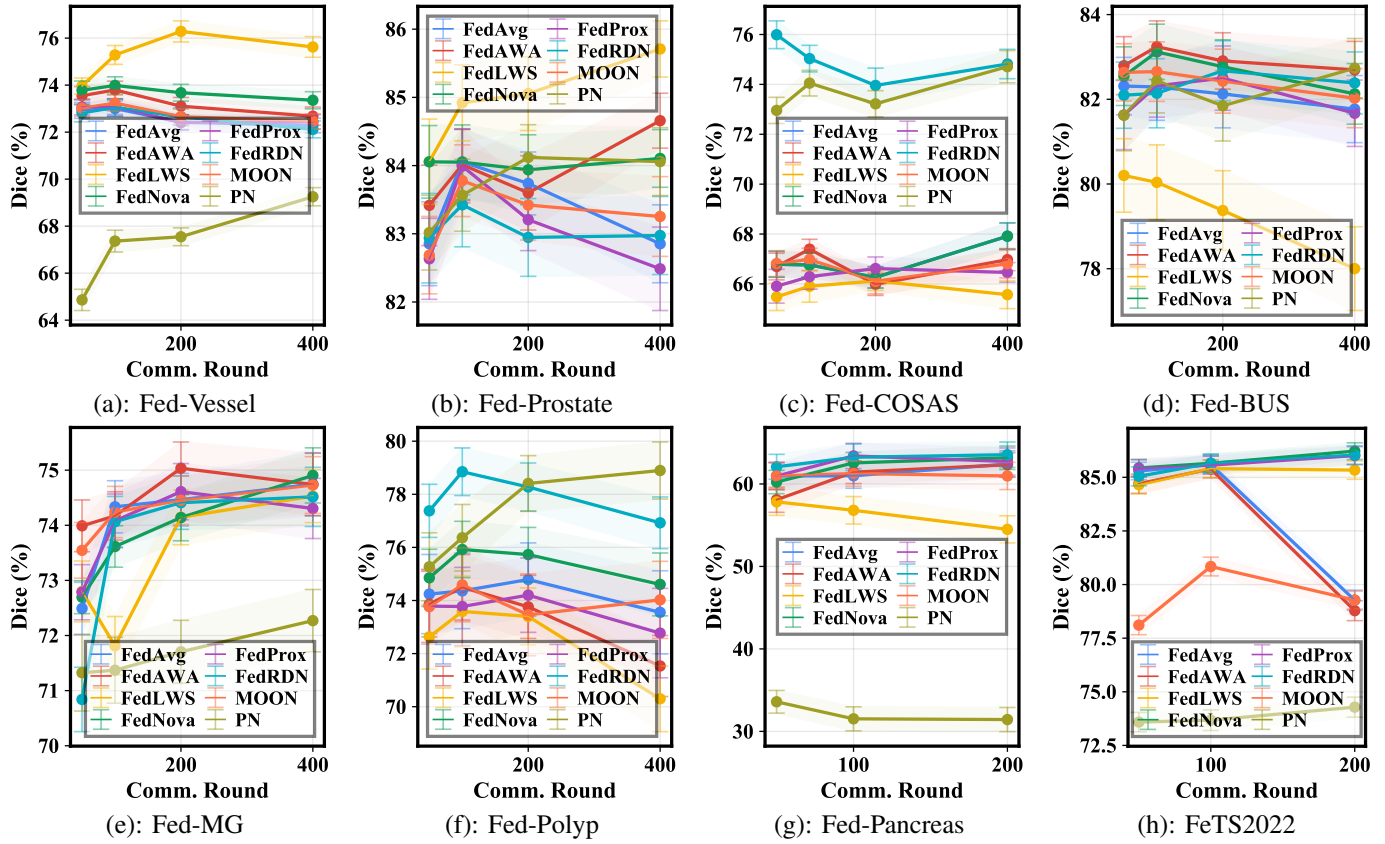


Fig. 2: The segmentation performance of different gFL methods with different communication rounds on 2D and 3D datasets.

(89.22%), C6 (80.74%), and tying for best on C2 (88.78%) and C4 (82.98%). This reaffirms the value of client-specific batch normalization statistics in capturing domain-specific intensity distributions in MRI. SioBN delivers the highest score on C7 (86.19%) and ties on C9 (88.56%), demonstrating its effectiveness. FedPer secures the best result on C8 (90.98%), highlighting the benefit of personalized feature extractors. Ditto and FedRoD performed poorly across multiple clients. In particular, Ditto falls behind on C5 (78.95%) and C9 (82.34%), suggesting that its dual-model personalization may limit beneficial knowledge transfer in larger-scale federations.

### B. Generalization

To assess the practical applicability of gFL methods in real-world clinical scenarios, we evaluate their generalization capability on five unseen datasets spanning diverse imaging modalities: ARIA [66] and IOSTAR [67] (vessel segmentation with fundus images), MSD-prostate [68] (prostate segmentation with MRI images), Kvasir-SEG [69] (polyp segmentation with endoscopic images), and BUS [70] (breast tumor segmentation with ultrasound images). These datasets are entirely held out during training, serving as a rigorous test of each method’s ability to segment images from previously unseen domains without any fine-tuning.

As shown in Table X, FedLWS demonstrates remarkable generalization on three of the five datasets, achieving the highest Dice scores on ARIA (66.41%), IOSTAR (72.40%), and MSD (84.27%). Its adaptive weighting mechanism appears

to learn representations that transfer well to unseen fundus and organ segmentation tasks. However, FedLWS catastrophically fails on Kvasir-SEG, plummeting to only 20.69%, with a high variance. The marked performance collapse indicates that the method over-optimizes for the specific feature distributions during federation, which in turn narrows its generalizability and leads to failure on unseen endoscopic data. This result serves as an important caution against deploying adaptive weighting strategies without comprehensive out-of-distribution (OOD) validation. PN exhibits the strongest performance on Kvasir-SEG (74.17%) and competitive results on BUS (74.15%) and MSD (83.72%). Its learnable global normalization statistics seem to capture domain-invariant features beneficial for endoscopic and ultrasound images, though it lags behind on retinal datasets (ARIA: 60.71%, IOSTAR: 59.51%). The method’s stability across most OOD tasks is noteworthy, but its moderate performance on fundus data indicates limitations in handling domain shifts characterized by fine vessel structures. FedAWA and FedNova deliver consistently mid-to-high performance across all five datasets, with FedAWA slightly edging out others on BUS (74.54%). Their balanced generalization suggests that simple aggregation with adaptive weighting or normalized averaging provides a reasonable trade-off between fitting training domains and retaining OOD robustness. FedAvg, FedProx, and MOON demonstrated similar performance profiles, with Dice scores clustering within a narrow range of 63~74% across most datasets. This consistency suggests that conventional FL meth-

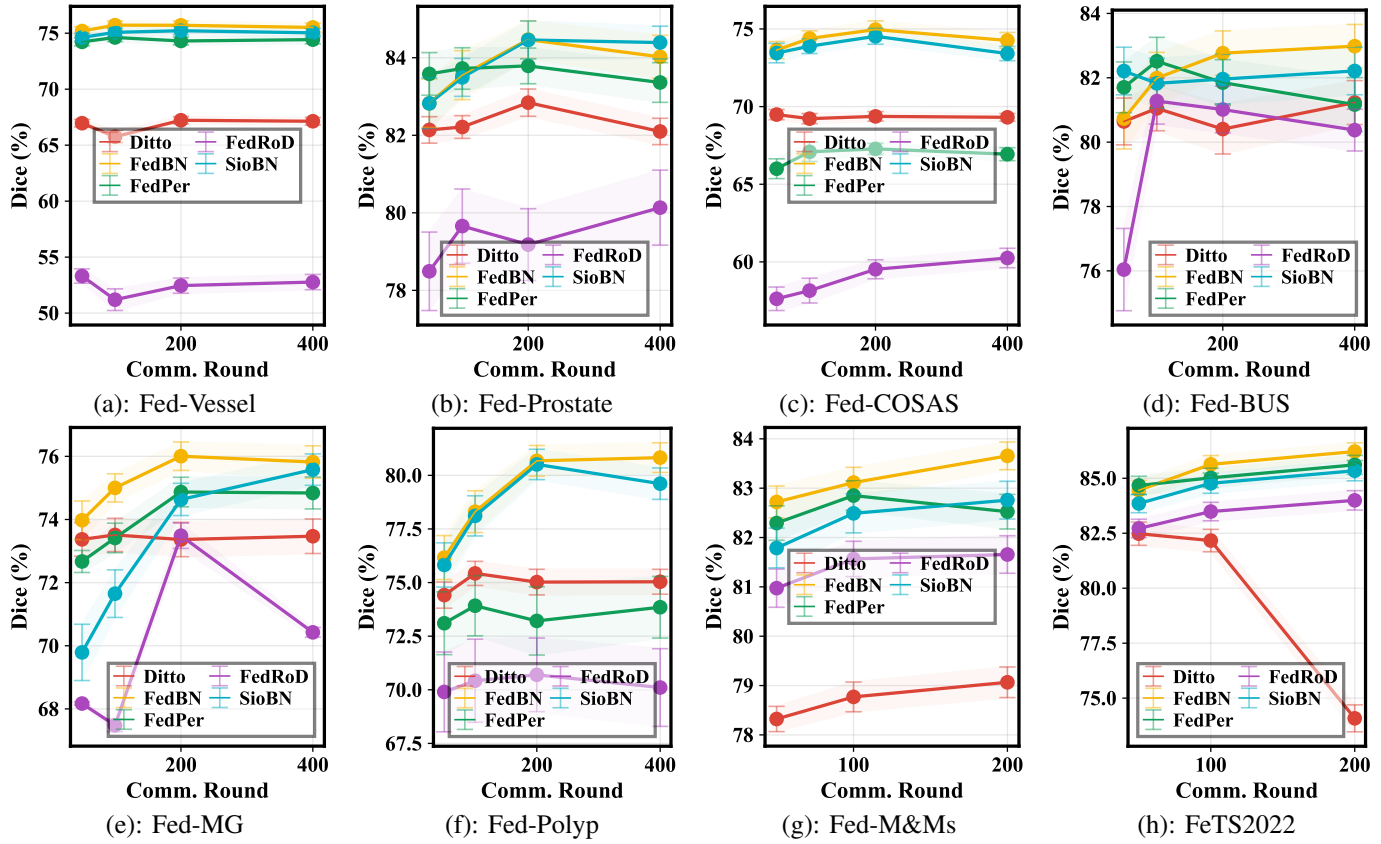


Fig. 3: The segmentation performance of different pFL method with different communication rounds on 2D and 3D datasets.

ods provide a moderate, yet reliable, level of generalization, though they do not exhibit a clear advantage when adapting to any specific unseen domain.

C. Effect of Communication Frequency

To investigate the impact of communication frequency on federated learning performance, we evaluate various FL algorithms on nine medical image segmentation datasets under varying communication rounds and local update frequencies, as shown in Figs. 2 and 3. For the six datasets (Fed-Vessel, Fed-Prostate, Fed-COSAS, Fed-BUS, Fed-MG, and Fed-Polyp), the total number of training epochs is fixed at 400, meaning that as the number of communication rounds decreases from 400 to 50, the number of local epochs per round correspondingly increases from 1 to 8. For the three datasets (Fed-Pancreas, Fed-M&MS and FeTS2022), the total epochs are 200, with local epochs per round increasing from 1 to 4 as communication rounds decrease from 200 to 50. This experimental design allows us to investigate the trade-off between communication frequency and local computation, and to assess the robustness of each FL method to different degrees of model staleness and client drift.

1) Effect of Communication Frequency for gFL Methods:

As illustrated in Fig. 2, most methods achieve comparable performance on Fed-Vessel, with FedLWS and FedNova showing a slight edge across all communication settings. FedLWS attains the highest accuracy at 400 rounds and maintains competitive performance as rounds decrease, though it experiences

a gradual decline at 50 rounds. In comparison, PN exhibits a marked sensitivity to communication constraints, with its performance collapsing sharply to 64.86% at 50 rounds. FedAWA and FedProx exhibit stable behavior with minimal degradation when local epochs increase. Fed-Prostate offers a different perspective on algorithm behavior. Although FedLWS achieves the best performance across different communication frequencies, its performance demonstrates a clear downward trend as the communication frequency decreases. Similarly, FedAWA exhibits this same pattern of decline. In contrast, FedNova exhibited highly stable performance across different communication frequencies. The other methods (FedAvg, MOON, FedRDN and FedProx) exhibited a counterintuitive phenomenon: higher communication frequencies led to lower performance. This pattern was also observed on the Fed-BUS dataset, with all methods except PN following this trend. The results on Fed-COSAS reveal a stark contrast between methods. FedRDN and PN both achieve superior performance compared to all other Fed methods; however, they respond differently to communication constraints. The performance of FedRDN improves with fewer communication rounds, while PN’s performance declines under the same conditions. The remaining methods, including FedAvg, FedAWA, FedLWS, FedNova, FedProx, and MOON, all fall within the 65~68% range, with little variation across different communication rounds.

On the Fed-MG dataset, nearly all methods exhibit a consistent trend: segmentation performance improves as com-

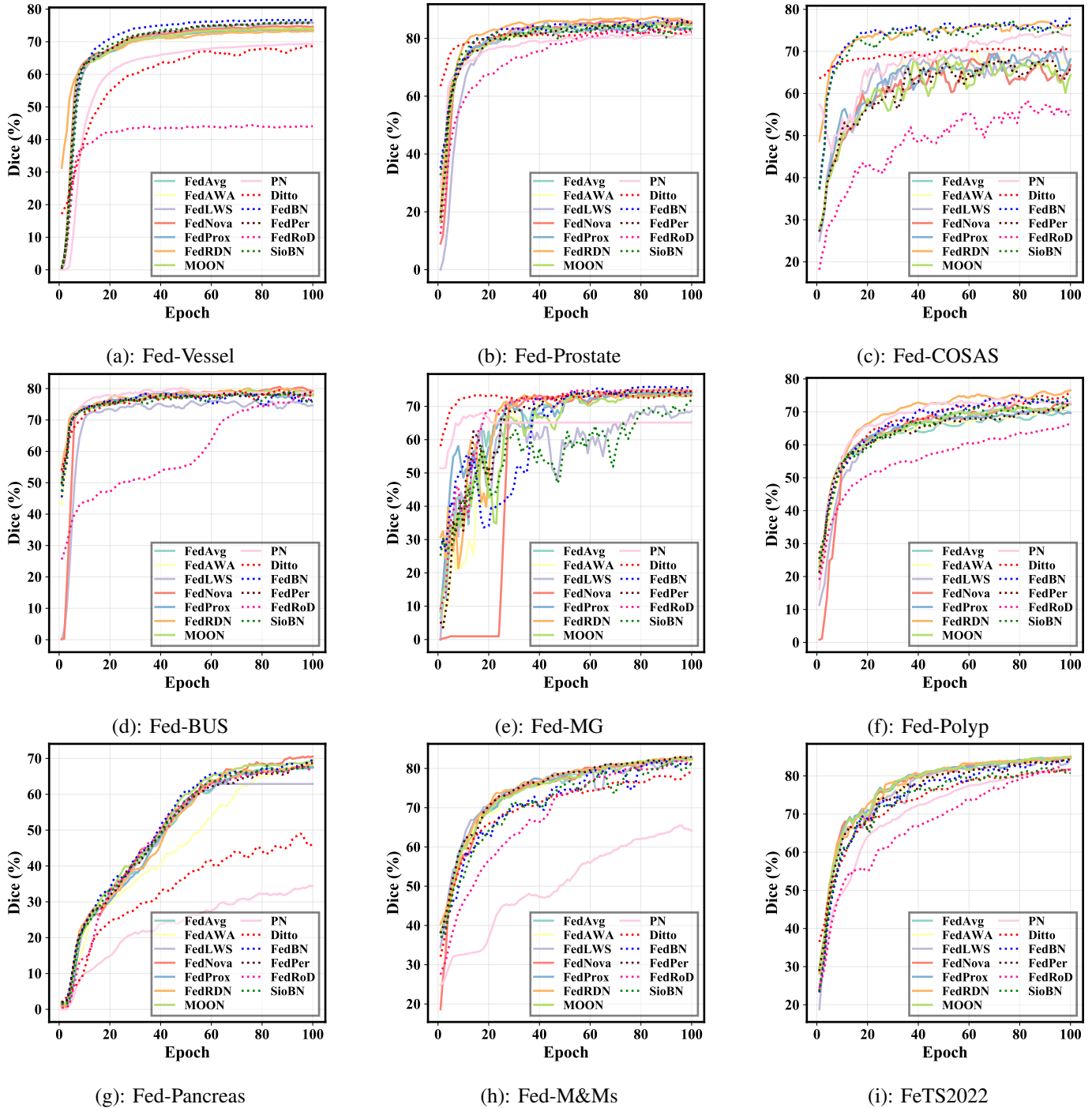


Fig. 4: The convergence behaviors of different FL methods 2D and 3D datasets.

munication frequency increases. Notably, FedRDN suffers a substantial performance degradation when the communication frequency is extremely low. The Fed-Polyp dataset presents a unique pattern. As communication frequency decreases, all methods except PN—which shows a declining trend—exhibits an initial performance improvement followed by a subsequent drop. FedRDN, FedAWA, and FedLWS, in particular, experiences notable performance degradation. This suggests that, in federated learning settings, more frequent communication does not necessarily translate to better performance. On

the Fed-Pancreas and FeTS2022 datasets, FedRDN, FedProx, and FedNova all demonstrate low sensitivity to variations in communication frequency. In contrast, PN and FedLWS exhibit opposing performance trends across the two datasets: their performance improves slightly as the communication frequency decreases on Fed-Pancreas, but shows a mild decline on FeTS2022. Meanwhile, FedAWA and FedAvg remain highly stable on Fed-Pancreas, yet achieve substantially lower performance on FeTS2022 when the communication frequency is high.

2) *Effect of Communication Frequency for pFL Methods:* As shown in Fig. 3, pFL methods demonstrated minimal performance fluctuation on Fed-Vessel across varying communication frequencies. Notably, FedBN and SioBN consistently achieve the highest Dice scores regardless of the communication setting. This indicates that methods incorporating batch normalization (FedBN and SioBN) exhibit robustness to the trade-off between communication frequency and local update steps. On Fed-Prostate, as communication frequency decreases, FedRoD exhibits an overall downward trend, while the other pFL methods first increase and then decline. On Fed-COSAS and Fed-BUS, FedBN, FedPer, and Ditto exhibit minimal performance fluctuation as communication frequency vary, while FedRoD shows an overall downward trend. On Fed-MG, Ditto stands out as the only method that maintains stable performance across communication frequencies, whereas most other methods show a pronounced decline as frequency decreases. On the Fed-MG, Fed-M&Ms, and FeTS2022 datasets, with the exception of Ditto, all other methods exhibit a marked downward trend as communication frequency decreases. In contrast, Ditto exhibits a completely different performance trend across these three datasets. In Fed-Polyp, FedBN and SioBN again lead with scores above 80% at high communication frequency, but both exhibit a clear downward trend as rounds decrease: FedBN drops from 80.83% at 400 rounds to 76.16% at 50 rounds, and SioBN from 80.51% at 200 rounds to 75.82% at 50 rounds. The remaining methods, however, demonstrate remarkable stability across communication rounds. Overall, among these pFL methods, FedBN consistently achieves the best performance across different communication frequencies, while also exhibiting a clear downward trend as communication frequency decreases.

#### D. Analysis of Convergence Behaviors

To investigate the convergence behaviors of various FL methods on different medical datasets, we plot their Dice scores of validation sets against the number of training epochs, as shown in Fig. 4. The number of communication rounds  $T$  is set to 100 for all datasets.

On the Fed-Vessel dataset, all methods exhibit a rapid performance increase in the first 30 epochs, followed by a gradual plateau. pFL approaches (FedBN, FedPer, SioBN) achieve the highest final Dice scores, marginally outperforming gFL methods (FedAvg, FedProx, FedNova, FedAWA, FedLWS, MOON) which cluster around 73~75%. FedRDN shows an anomalously high initial score (around 31%) but converges similarly to gFL methods. In contrast, PN and Ditto converge to notably lower scores, while FedRoD exhibits severe degradation, plateauing at only around 44% Dice, indicating poor suitability for this task. For the Fed-Prostate dataset, FedRDN achieves the highest final Dice, demonstrating superior convergence. FedBN, FedPer, and SioBN also reach competitive levels but exhibit moderate fluctuations. Traditional methods (FedAvg, FedProx, FedNova, MOON, FedAWA) cluster together and converge smoothly. FedLWS starts from near zero but catches up after 40 epochs, eventually matching these traditional methods. Ditto begins with an unusually high initial

score yet shows limited growth, plateauing at about 82%. FedRoD underperforms significantly, converging to only 83% despite steady progress.

On the Fed-COSAS dataset as illustrated in Fig. 4(e), FedRDN, FedBN, and SioBN achieve the highest Dice scores with rapid initial improvement and stable convergence after around 60 epochs. Their curves are smooth and exhibit minimal fluctuations, indicating robust optimization. FedAvg, FedNova, FedProx, FedAWA, and FedPer follow a similar trend: steady but slower improvement. They display noticeable oscillations throughout training, particularly in the later stages, suggesting sensitivity to data heterogeneity. FedRoD lags significantly behind all others, peaking at only around 56%, with a slow and unstable increase. On the Fed-BUS dataset, FedLWS starts from a near-zero Dice but catches up swiftly, reaching over 70% by epoch 30 and maintaining competitive performance thereafter, indicating its strong adaptability despite poor initialization. FedNova also shows a sharp rise after epoch 10, achieving high scores early and continuing to improve steadily. FedAvg, FedAWA, FedProx, FedRDN, MOON, FedBN, FedPer, and SioBN follow similar smooth trajectories, starting at 45~55% and converging to 76~79% with minor fluctuations. These methods demonstrate robust and balanced convergence, with FedAWA and MOON slightly outperforming FedAvg in later stages. FedProx and FedRDN exhibit moderate oscillations but remain within the same performance band. FedRoD progresses slowly but consistently, ending near 76.40%, indicating slower yet steady convergence.

On the Fed-MG dataset, gradual and stable convergence is observed for FedAvg, FedProx, MOON, FedPer, and FedRoD. Among them, FedPer and FedRoD ascend slightly faster and reach marginally higher plateaus, indicating effective personalization or regularisation. FedAWA, FedRDN, and FedBN also progress steadily but ultimately achieve the top Dice scores. FedBN, in particular, exhibits the highest final value with very low variance after convergence, suggesting robust feature representation via batch normalization. On the Fed-Polyp dataset, FedRDN demonstrates the fastest convergence and attains the highest final Dice score, maintaining stable performance after around 60 epochs. Ditto and SioBN also achieve strong final results but with mild fluctuations in later stages. In contrast, FedAvg and FedProx converge more slowly and plateau at lower accuracies, indicating limited effectiveness in this task. Notably, FedRoD lags behind all other methods, with the slowest convergence and the lowest final Dice score, suggesting it is less suitable for this dataset. On the Fed-Pancreas dataset, most methods demonstrate smooth and steady convergence, with minimal oscillation after 60 epochs. PN and Ditto converge slowly and remain at a relatively low level. On the Fed-M&MS and FeTS2022 datasets, except for PN, gFL methods demonstrate rapid and steady improvement, converging to high-performance plateaus with minimal fluctuations. PN exhibits the slowest growth, particularly on the Fed-M&MS dataset. Among pFL approaches, FedPer achieves the highest final segmentation performance, while maintaining smooth convergence throughout training on the two datasets. The others exhibit pronounced oscillations during training.

TABLE XI: Fairness study of different FL methods on Fed-Vessel, Fed-Prostate, Fed-Polyp and Fed-COSAS (%).

Methods	Fed-Vessel			Fed-Prostate			Fed-Polyp			Fed-COSAS		
	aDice↑	Std↓	wDice↑									
<i>Generic FL methods</i>												
FedAvg	73.01	3.28	68.50	84.05	4.80	76.35	74.36	14.23	49.68	66.76	4.84	60.14
FedAWA	73.79	3.73	68.45	84.01	5.26	74.84	74.49	12.32	53.55	67.39	3.96	61.82
FedLWS	<b>75.28</b>	4.01	<b>70.24</b>	<b>84.92</b>	5.56	74.49	73.58	13.32	49.38	65.90	6.38	57.11
FedNova	73.98	3.68	68.86	84.05	5.46	74.94	75.92	10.60	58.79	66.76	4.84	60.14
FedProx	73.07	<b>3.24</b>	68.56	83.99	5.37	76.00	73.77	14.73	47.57	66.29	5.01	59.25
FedRDN	73.05	3.68	67.81	83.42	6.15	71.92	<b>78.85</b>	8.95	65.85	<b>75.03</b>	5.32	67.60
MOON	73.23	3.40	68.79	83.77	5.25	75.26	74.58	13.89	50.71	66.98	4.52	61.29
PN	67.36	4.63	57.94	83.56	5.27	75.24	76.36	12.52	52.99	74.05	5.14	<b>67.79</b>
<i>Personalized FL methods</i>												
Ditto	65.75	5.33	55.79	82.21	<b>2.93</b>	<b>77.83</b>	75.42	<b>5.62</b>	<b>68.07</b>	69.22	<b>3.26</b>	64.64
FedBN	75.71	3.84	69.62	83.55	6.31	73.86	78.30	9.75	60.19	74.38	4.91	67.64
FedPer	74.61	3.64	68.65	83.72	5.35	75.96	73.91	14.03	49.52	67.08	6.25	58.24
FedRoD	51.19	9.68	36.99	79.65	9.56	62.38	70.42	19.36	33.98	58.15	7.98	50.61
SioBN	75.08	3.71	69.08	83.49	4.89	76.03	78.11	9.36	62.76	73.89	4.74	67.34

TABLE XII: Fairness study of different FL methods on Fed-BUS, Fed-Pancreas, Fed-M&amp;Ms and FeTS2022 (%).

Methods	Fed-BUS			Fed-Pancreas			Fed-M&Ms			FeTS2022		
	aDice↑	Std↓	wDice↑	aDice↑	Std↓	wDice↑	aDice↑	Std↓	wDice↑	aDice↑	Std↓	wDice↑
<i>Generic FL methods</i>												
FedAvg	80.62	7.98	71.90	60.98	15.10	33.97	82.42	3.54	79.00	85.59	4.07	78.40
FedAWA	<b>81.81</b>	<b>6.02</b>	<b>74.89</b>	61.42	13.81	36.68	82.25	3.60	78.75	85.38	4.15	77.60
FedLWS	77.80	8.55	68.59	56.80	16.65	26.44	82.32	3.41	79.52	85.40	4.07	77.68
FedNova	81.66	6.53	73.44	62.55	<b>12.73</b>	<b>41.83</b>	82.54	3.37	79.01	<b>85.65</b>	4.10	78.11
FedProx	80.65	7.39	72.52	<b>63.39</b>	15.28	34.43	82.50	3.49	79.30	85.56	4.18	<b>78.63</b>
FedRDN	80.43	8.28	71.34	63.23	16.13	32.99	82.54	3.57	76.92	<b>85.65</b>	4.27	77.71
MOON	81.07	7.02	73.88	61.26	15.38	33.37	82.24	3.53	78.40	80.83	4.35	73.07
PN	80.80	7.64	73.04	31.52	14.56	9.52	60.06	5.13	54.37	73.67	4.81	66.00
<i>Personalized FL methods</i>												
Ditto	79.23	6.63	71.64	45.92	24.77	14.60	78.77	3.01	74.75	82.16	5.09	75.95
FedBN	80.40	8.19	70.62	60.98	15.89	34.36	<b>83.11</b>	3.09	78.81	85.63	<b>3.98</b>	77.71
FedPer	81.06	7.64	73.36	62.31	15.75	33.60	82.85	<b>2.98</b>	<b>80.14</b>	85.01	4.38	77.18
FedRoD	79.51	6.96	73.03	61.94	16.44	31.48	81.56	3.57	78.00	83.48	4.20	76.36
SioBN	80.20	7.88	71.71	61.83	15.74	33.89	82.49	3.96	75.77	84.77	4.53	75.79

### E. Fairness Study

In federated learning, fairness is a critical consideration, measuring the variability in model performance across different clients. To comprehensively evaluate the fairness of each method, we use three metrics: the equally weighted average of Dice scores (aDice) across all clients, the standard deviation (Std) of client performance (where lower values indicate greater fairness), and the worst-client Dice score (wDice) representing the performance of the worst-performing client, which serves as a direct indicator of fairness. This section provides a detailed analysis of the fairness characteristics of eight generic FL approaches (FedAvg, FedAWA, FedLWS, FedNova, FedProx, FedRDN, MOON, and PN) and five personalized FL approaches (Ditto, FedBN, FedPer, FedRoD, and SioBN) across eight medical image segmentation datasets. The fairness performance of these methods is demonstrated in Tables XI and XII.

1) *Fairness Analysis of gFL Methods:* Among the gFL methods, FedRDN demonstrates the most balanced fairness. On the Fed-Polyp dataset, FedRDN achieves the highest aDice (78.85%), the lowest Std (8.95), and the highest wDice (65.85%), significantly outperforming other methods. Similarly, on Fed-COSAS, its aDice (75.03%), Std (5.32), and wDice (67.60%) are among the best. This suggests that Fe-

dRDN effectively mitigates client drift and enhances fairness. FedNova also performs well across multiple datasets; for instance, on Fed-Polyp, it attains an aDice of 75.92%, a Std of 10.60, and a wDice of 58.79%, with comprehensive performance second only to FedRDN. In contrast, FedLWS and FedProx show greater volatility in fairness: FedLWS achieves a high aDice (75.28%) and a relatively good wDice (70.24%) on Fed-Vessel, but on Fed-Pancreas, its aDice drops to 56.80%, wDice plummets to 26.44%, and Std soars to 16.65, indicating sensitivity to heterogeneity. MOON and PN exhibit severe degradation on some datasets: PN's aDice is merely 31.52% on Fed-Pancreas, with a wDice as low as 9.52%.

2) *Fairness Analysis of pFL Methods:* Personalized FL methods aim to tailor models for each client, theoretically reducing Std and improving wDice. Ditto stands out as a prime example: on Fed-Prostate, Ditto achieves the lowest Std (2.93) among all methods and the highest wDice (77.83%), although its aDice (82.21%) is slightly lower than some generic methods. On Fed-Polyp, Ditto maintains a remarkably low Std of 5.62 and a high wDice of 68.07%, while keeping aDice (75.42%) at a respectable level. This indicates that Ditto's local personalization effectively protects underperforming clients, significantly enhancing fairness. FedBN leverages batch normalization statistics to adapt to client distributions, achieving

the highest aDice (75.71%) and a competitive wDice (69.62%) on Fed-Vessel, accompanied by a low Std (3.84). On Fed-M&Ms, FedBN’s aDice (83.11%) and Std (3.09) are among the best. FedPer and SioBN show similar performance but offer limited fairness improvements on highly heterogeneous datasets like Fed-Pancreas. Notably, FedRoD performs the worst across all datasets, with its aDice, Std, and wDice lagging significantly behind other methods, suggesting its dual-classifier design may be unsuitable for medical image segmentation tasks.

## V. DISCUSSION

### A. Discussion on Segmentation Performance

Tables III-IX present a comprehensive evaluation of 13 FL methods across 9 medical image segmentation tasks, encompassing diverse imaging modalities (such as fundus, ultrasound, colonoscopy, infrared, and MRI) and heterogeneous data distributions. The results reveal several important insights regarding the behavior of generic and personalized FL approaches in medical imaging contexts.

The local training paradigm, where models are trained independently on each client without any federation, establishes a critical reference point. Notably, local training achieves competitive performance in several datasets, particularly on Fed-Vessel (*e.g.*, 78.41% on C5) and Fed-Prostate (*e.g.*, 86.74% on C5). This observation underscores the substantial statistical heterogeneity inherent in medical imaging data, where client-specific distributions can diverge significantly, making naive federation potentially detrimental. *The strong local performance motivates the need for personalized approaches that can leverage cross-client knowledge while preserving client-specific features.* Among generic FL methods, which aim to learn a single global model, we observe considerable variability. FedLWS consistently demonstrates robust performance, achieving the highest results among generic methods on Fed-Vessel and Fed-Prostate, suggesting its adaptive weighting mechanism effectively mitigates client drift. FedRDN also shows strong results, particularly on Fed-COSAS (77.67% on C1) and Fed-Pancreas (74.37% on C2), indicating its domain gap elimination strategy benefits generalization across highly heterogeneous domains. However, conventional methods like FedAvg and FedProx frequently underperform relative to Local baselines, especially on severely heterogeneous datasets such as Fed-Vessel and Fed-Pancreas. This confirms that standard aggregation protocols are susceptible to performance degradation under non-IID conditions common in medical imaging. The poor performance of PN across nearly all datasets further highlights the risks of aggressive normalization strategies that may discard valuable client-specific statistical information.

*Personalized FL methods, which retain client-specific parameters or adapt the global model locally, consistently outperform generic approaches.* FedBN emerges as the most robust method overall, achieving top-tier performance on 7 out of 9 datasets, including Fed-Vessel, Fed-BUS, Fed-MG, Fed-Polyp, and FeTS2022. By maintaining local batch normalization statistics while sharing convolutional layers, FedBN effectively captures domain-specific feature distributions without

sacrificing collaborative representation learning. This design choice proves particularly advantageous for medical imaging, where intensity distributions and texture patterns vary substantially across institutions due to differing acquisition protocols. SioBN and FedPer also demonstrate competitive performance, frequently ranking among the top two methods on datasets such as Fed-M&Ms and Fed-Pancreas. SioBN’s client-specific affine parameters offer a lightweight personalization mechanism that balances communication efficiency and model fidelity. FedPer’s feature extractor sharing with personalized classifiers provides flexibility, though it exhibits higher variance on smaller datasets (*e.g.*, Fed-COSAS). The collective results underscore that no single FL method dominates universally; however, *FedBN and its variants (SioBN) provide consistently superior and stable performance across a broad spectrum of medical imaging tasks.* The integration of domain-specific normalization layers emerges as a simple yet powerful inductive bias for handling cross-institutional heterogeneity. Future work should explore adaptive personalization strategies that dynamically allocate client-specific capacity based on task difficulty and domain distance.

### B. Discussion on Generalization Performance

The generalization evaluation on five unseen datasets in Table X reveals a critical relationship between a method’s ability to generalize across participating clients and its performance on unseen domains. Notably, FedLWS exhibits a strong positive correlation: on Fed-Vessel and Fed-Prostate, where it achieves the highest segmentation accuracy across most clients (see Tables III and IV), it also attains the best generalization results on unseen fundus datasets (ARIA and IOSTAR) and the unseen prostate dataset (MSD). Conversely, on Fed-Polyp, where FedLWS delivers among the poorest performance on participating clients, as shown in Table VI(b), it catastrophically fails on the unseen endoscopic dataset Kvasir-SEG, plummeting to only 20.69% Dice. This consistent pattern suggests that *a method’s generalization to unseen domains is strongly tied to its ability to perform well across the participating clients—when it excels on seen clients, it tends to transfer better; when it underperforms on seen clients, it is unlikely to generalize.* This observation challenges the conventional assumption that optimizing for seen clients necessarily leads to overfitting and poor out-of-distribution (OOD) performance. It also provides an important insight for domain generalization in federated learning: rather than solely focusing on explicit domain generalization techniques for unseen sites, *an alternative and potentially more direct pathway is to enhance the model’s generalization capability on the participating clients themselves.* In other words, designing FL algorithms that achieve high and balanced performance across heterogeneous in-distribution clients may implicitly equip the model with representations that are robust to unseen domains. Additionally, methods like FedAvg, FedProx, and MOON exhibit moderate but stable performance across all five unseen datasets. While they never achieve top results, they also avoid catastrophic failures, making them safer choices in heterogeneous clinical environments where the target domain cannot be predetermined.

### C. Discussion on Communication Frequency

From Figs. 2 and 3, we observe that the impact of reducing communication rounds (*i.e.*, increasing local updates per round) is highly dependent on both the dataset and the specific FL method. For generic FL approaches, methods such as FedAvg, FedProx, and FedNova generally maintain stable performance across different round settings on most datasets, indicating that they can tolerate a certain degree of local overfitting when communication is limited. However, their performance occasionally degrades when local epochs become too large (*e.g.*, at 50 rounds), suggesting that excessive local updating may lead to client drift, particularly under severe data heterogeneity. In contrast, FedLWS and FedRDN exhibit more pronounced fluctuations, sometimes achieving superior results at intermediate round numbers but falling behind when rounds are extremely scarce. This behavior implies that these methods are more sensitive to the balance between local and global optimization, and their convergence may require a minimum number of communication steps. From a broader perspective, our findings underscore the importance of considering the communication–performance trade-off when deploying FL in real-world medical applications, where bandwidth constraints often limit the number of permissible rounds. Methods that preserve high accuracy even with infrequent communication—such as FedBN and SioBN—are particularly attractive for such settings. Moreover, the dataset-dependent variability in method rankings emphasizes that no single FL algorithm universally dominates; instead, the choice should be guided by the expected data heterogeneity and the available communication budget. Future research could explore adaptive strategies that dynamically adjust local update steps based on estimated heterogeneity or communication resource availability. Additionally, combining the strengths of normalization-based personalization with robust aggregation techniques may yield further improvements.

### D. Discussion on Fairness

Based on the comprehensive experimental results presented in Tables XI and XII, several important observations can be drawn regarding the fairness characteristics of federated learning methods in medical image segmentation tasks. First, a clear trade-off is observed between gFL methods and pFL methods. pFL methods like Ditto achieve the lowest standard deviation on several datasets (*e.g.*, 2.93 on Fed-Prostate, 5.62 on Fed-Polyp, 3.26 on Fed-COSAS) and the highest worst-client Dice scores (77.83% on Fed-Prostate, 68.07% on Fed-Polyp), but this often comes at the cost of average performance. For example, on Fed-Prostate, Ditto’s average Dice (82.21%) is lower than that of FedAvg (84.05%) and FedLWS (84.92%). This suggests that enhancing the performance of the worst-performing clients through personalization may involve a trade-off with slightly reduced overall average performance. Second, method performance varies significantly across different datasets. On datasets like Fed-Vessel and Fed-M&Ms, most methods achieve relatively high average Dice scores and low standard deviations. In contrast, on datasets like Fed-Pancreas and Fed-Polyp, all methods exhibit substantially higher stan-

dard deviations and lower worst-client Dice scores. For instance, even the best-performing method on Fed-Pancreas (FedProx, with an average Dice of 63.39%) suffers from a high standard deviation of 15.28 and a low worst-client Dice of only 34.43%, indicating that certain datasets pose greater inherent challenges to achieving fairness. Across the eight datasets, FedRDN, FedNova, and FedBN demonstrate the most consistent fairness performance, frequently ranking among the top methods in terms of both standard deviation and worst-client Dice. FedAWA also shows robust performance, particularly on Fed-BUS where it achieves the best average Dice, lowest standard deviation, and highest worst-client Dice. Conversely, FedRoD and PN exhibit the least stable fairness characteristics, with performance deteriorating sharply on specific datasets. These observations have practical implications for method selection: *if safeguarding the worst-performing clients is the primary concern (e.g., requiring all participating institutions to achieve acceptable performance), personalized methods like Ditto are preferable, despite a potential minor reduction in average performance; if pursuing high overall accuracy while maintaining fairness, FedRDN and FedBN emerge as superior choices.* Although existing methods have made progress, on challenging datasets like Fed-Pancreas, all methods exhibit standard deviations exceeding 12 and worst-client Dice scores below 42%, indicating that the fairness problem is not yet fully resolved. Future research could explore hybrid strategies that integrate the strengths of both gFL and pFL methods—for example, combining FedRDN’s heterogeneity reduction with Ditto’s local personalization—to simultaneously optimize average performance and fairness. Additionally, investigating adaptive mechanisms that dynamically adjust the degree of personalization based on detected client heterogeneity could yield methods that automatically balance the trade-off between overall accuracy and worst-client performance.

## VI. CONCLUSION

In this paper, we introduced FL-MedSegBench, the first comprehensive benchmark for federated learning in medical image segmentation. Our benchmark encompasses nine diverse medical segmentation tasks spanning ten imaging modalities across both 2D and 3D formats, with realistic non-IID data partitions that mirror real-world clinical heterogeneity. We systematically evaluated eight generic FL methods and five personalized FL methods, assessing not only segmentation accuracy but also fairness, communication efficiency, convergence behavior, and generalization to unseen clients.

Our extensive experiments yield several key findings. First, personalized FL methods, particularly those incorporating client-specific batch normalization statistics (*e.g.*, FedBN), consistently outperform generic approaches across most datasets, demonstrating the critical importance of adapting to local data distributions while preserving collaborative knowledge sharing. Second, no single FL method dominates universally; performance is highly dataset-dependent, with methods such as FedRDN and FedLWS excelling on specific tasks while underperforming on others. Third, communication frequency analysis reveals that the optimal trade-off between

communication frequency and local computation varies substantially across datasets and methods, with normalization-based personalization methods (FedBN, SioBN) exhibiting remarkable robustness to reduced communication. Fourth, generalization assessment uncovers a critical relationship: a method’s generalization to unseen domains is strongly tied to its ability to perform well across participating clients. This finding challenges the conventional assumption that optimizing for seen clients necessarily leads to overfitting and poor out-of-distribution performance, suggesting instead that enhancing model performance on participating clients themselves may offer a more direct pathway to robust domain generalization.

Our work provides foundational insights and practical guidelines for deploying FL in real-world medical imaging applications. The open-source benchmark toolkit, including standardized datasets, implementations, and evaluation protocols, aims to foster reproducible research and accelerate the development of more robust, efficient, and clinically applicable federated learning solutions. Future research directions include exploring adaptive personalization strategies that dynamically allocate client-specific capacity based on task difficulty, developing aggregation methods with stronger theoretical guarantees for OOD generalization, and integrating fairness constraints with personalization mechanisms to better protect all participating institutions.

## REFERENCES

- [1] D.-P. Fan, G.-P. Ji, T. Zhou, G. Chen, H. Fu, J. Shen, and L. Shao, “Pranet: Parallel reverse attention network for polyp segmentation,” in *MICCAI*. Springer, 2020, pp. 263–273.
- [2] M. Zhu, Z. Chen, and Y. Yuan, “Dsi-net: Deep synergistic interaction network for joint classification and segmentation with endoscope images,” *IEEE Transactions on Medical Imaging*, vol. 40, no. 12, pp. 3315–3325, 2021.
- [3] S. Zhong, W. Wang, Q. Feng, Y. Zhang, and Z. Ning, “Cross-view discrepancy-dependency network for volumetric medical image segmentation,” *Medical Image Analysis*, vol. 99, p. 103329, 2025.
- [4] X. Huang, C. Yue, Y. Guo, J. Huang, Z. Jiang, M. Wang, Z. Xu, G. Zhang, J. Liu, T. Zhang *et al.*, “Multidimensional directionality-enhanced segmentation via large vision model,” *Medical Image Analysis*, vol. 101, p. 103395, 2025.
- [5] V. I. Butoi, J. J. G. Ortiz, T. Ma, M. R. Sabuncu, J. Guttag, and A. V. Dalca, “Universeg: Universal medical image segmentation,” in *ICCV*, 2023, pp. 21 438–21 451.
- [6] R. Azad, E. K. Aghdam, A. Rauland, Y. Jia, A. H. Avval, A. Bozorgpour, S. Karimijafarbigloo, J. P. Cohen, E. Adeli, and D. Merhof, “Medical image segmentation review: The success of u-net,” *IEEE Transactions on Pattern Analysis and Machine Intelligence*, vol. 46, no. 12, pp. 10076–10 095, 2024.
- [7] L. O. Gostin, L. A. Levit, and S. J. Nass, “Beyond the hipaa privacy rule: enhancing privacy, improving health through research,” 2009.
- [8] M. Goddard, “The eu general data protection regulation (gdpr): European regulation that has a global impact,” *International Journal of Market Research*, vol. 59, no. 6, pp. 703–705, 2017.
- [9] B. McMahan, E. Moore, D. Ramage, S. Hampson, and B. A. y Arcas, “Communication-efficient learning of deep networks from decentralized data,” in *AISTATS*, 2017, pp. 1273–1282.
- [10] M. Zhu, J. Liao, J. Liu, and Y. Yuan, “Fedoss: Federated open set recognition via inter-client discrepancy and collaboration,” *IEEE Transactions on Medical Imaging*, vol. 43, no. 1, pp. 190–202, 2024.
- [11] T. Li, A. K. Sahu, M. Zaheer, M. Sanjabi, and V. Smith, “Federated optimization in heterogeneous networks,” in *MLSys*, vol. 2, 2020, pp. 429–450.
- [12] M. Zhu, Z. Chen, and Y. Yuan, “Feddm: Federated weakly supervised segmentation via annotation calibration and gradient de-conflicting,” *IEEE Transactions on Medical Imaging*, vol. 42, no. 6, pp. 1632–1643, 2023.
- [13] B. Zhou, H. Xie, Q. Liu, X. Chen, X. Guo, Z. Feng, J. Hou, S. K. Zhou, B. Li, A. Rominger *et al.*, “Fedftn: Personalized federated learning with deep feature transformation network for multi-institutional low-count pet denoising,” *Medical Image Analysis*, vol. 90, p. 102993, 2023.
- [14] R. Jin and X. Li, “Backdoor attack and defense in federated generative adversarial network-based medical image synthesis,” *Medical Image Analysis*, vol. 90, p. 102965, 2023.
- [15] T. Li, A. K. Sahu, A. Talwalkar, and V. Smith, “Federated learning: Challenges, methods, and future directions,” *IEEE Signal Processing Magazine*, vol. 37, no. 3, pp. 50–60, 2020.
- [16] D. Yang, Z. Xu, W. Li, A. Myronenko, H. R. Roth, S. Harmon, S. Xu, B. Turkbey, E. Turkbey, X. Wang *et al.*, “Federated semi-supervised learning for covid region segmentation in chest ct using multi-national data from china, italy, japan,” *Medical Image Analysis*, vol. 70, p. 101992, 2021.
- [17] H. Guan, P.-T. Yap, A. Bozoki, and M. Liu, “Federated learning for medical image analysis: A survey,” *Pattern Recognition*, vol. 151, p. 110424, 2024.
- [18] S. Kim, H. Park, M. Kang, K. H. Jin, E. Adeli, K. M. Pohl, and S. H. Park, “Federated learning with knowledge distillation for multi-organ segmentation with partially labeled datasets,” *Medical Image Analysis*, vol. 95, p. 103156, 2024.
- [19] M. Li, P. Xu, J. Hu, Z. Tang, and G. Yang, “From challenges and pitfalls to recommendations and opportunities: Implementing federated learning in healthcare,” *Medical Image Analysis*, vol. 101, p. 103497, 2025.
- [20] Q. Li, B. He, and D. Song, “Model-contrastive federated learning,” in *CVPR*, 2021, pp. 10713–10722.
- [21] C. Shi, H. Zhao, B. Zhang, M. Zhou, D. Guo, and Y. Chang, “Fedawa: Adaptive optimization of aggregation weights in federated learning using client vectors,” in *CVPR*, 2025, pp. 30651–30660.
- [22] J. Wang, Q. Liu, H. Liang, G. Joshi, and H. V. Poor, “Tackling the objective inconsistency problem in heterogeneous federated optimization,” *NeurIPS*, vol. 33, pp. 7611–7623, 2020.
- [23] C. Shi, J. Li, H. Zhao, D. Guo, and Y. Chang, “Fedlws: Federated learning with adaptive layer-wise weight shrinking,” in *ICLR*, 2025.
- [24] Y. Zhang, F. Chen, Y. Qi, G. Yang, and H. Fu, “Pathfl: Multi-alignment federated learning for pathology image segmentation,” *Medical Image Analysis*, vol. 105, p. 103670, 2025.
- [25] Y. Yan, H. Fu, Y. Li, J. Xie, J. Ma, G. Yang, and L. Zhu, “A simple data augmentation for feature distribution skewed federated learning,” in *CVPR*, 2025, pp. 25 749–25 758.
- [26] A. Z. Tan, H. Yu, L. Cui, and Q. Yang, “Towards personalized federated learning,” *IEEE Transactions on Neural Networks and Learning Systems*, vol. 34, no. 12, pp. 9587–9603, 2022.
- [27] Z. Chen, M. Zhu, C. Yang, and Y. Yuan, “Personalized retrogress-resilient framework for real-world medical federated learning,” in *MICCAI*. Springer, 2021, pp. 347–356.
- [28] Z. Chen, C. Yang, M. Zhu, Z. Peng, and Y. Yuan, “Personalized retrogress-resilient federated learning toward imbalanced medical data,” *IEEE Transactions on Medical Imaging*, vol. 41, no. 12, pp. 3663–3674, 2022.
- [29] H. Liu, D. Wei, Q. Dai, X. Wu, Y. Zheng, and L. Wang, “Federated modality-specific encoders and partially personalized fusion decoder for multimodal brain tumor segmentation,” *Medical Image Analysis*, vol. 106, p. 103759, 2025.
- [30] M. G. Arivazhagan, V. Aggarwal, A. K. Singh, and S. Choudhary, “Federated learning with personalization layers,” *arXiv preprint arXiv:1912.00818*, 2019.
- [31] H.-Y. Chen and W.-L. Chao, “On bridging generic and personalized federated learning for image classification,” *ICLR*, 2022.
- [32] T. Li, S. Hu, A. Beirami, and V. Smith, “Ditto: Fair and robust federated learning through personalization,” in *ICML*. PMLR, 2021, pp. 6357–6368.
- [33] M. Andreux, J. O. du Terrail, C. Beguier, and E. W. Tramel, “Siloe federated learning for multi-centric histopathology datasets,” in *MICCAI Workshop on Domain Adaptation and Representation Transfer*. Springer, 2020, pp. 129–139.
- [34] X. Li, M. Jiang, X. Zhang, M. Kamp, and Q. Dou, “Fedbn: Federated learning on non-iid features via local batch normalization,” in *ICLR*, 2021.
- [35] J. Ogier du Terrail, S.-S. Ayed, E. Cyffers, F. Grimberg, C. He, R. Loeb, P. Mangold, T. Marchand, O. Marfoq, E. Mushtaq *et al.*, “Flamby: Datasets and benchmarks for cross-silo federated learning in realistic healthcare settings,” *NeurIPS*, vol. 35, pp. 5315–5334, 2022.
- [36] M. Manthe, S. Duffner, and C. Lartzien, “Federated brain tumor segmentation: An extensive benchmark,” *Medical Image Analysis*, vol. 97, p. 103270, 2024.

- [37] M. Zhu, Q. Yang, Z. Gao, Y. Yuan, and J. Liu, "Fedbm: Stealing knowledge from pre-trained language models for heterogeneous federated learning," *Medical Image Analysis*, vol. 102, p. 103524, 2025.
- [38] M. Zhu, Q. Yang, Z. Gao, J. Liu, and Y. Yuan, "Stealing knowledge from pre-trained language models for federated classifier debiasing," in *MICCAI*. Springer, 2024, pp. 685–695.
- [39] C. T. Dinh, N. Tran, and J. Nguyen, "Personalized federated learning with moreau envelopes," *NeurIPS*, vol. 33, pp. 21 394–21 405, 2020.
- [40] M. M. Fraz, P. Remagnino, A. Hoppe, B. Uyyanonvara, A. R. Rudnicka, C. G. Owen, and S. A. Barman, "An ensemble classification-based approach applied to retinal blood vessel segmentation," *IEEE Transactions on Biomedical Engineering*, vol. 59, no. 9, pp. 2538–2548, 2012.
- [41] S. Holm, G. Russell, V. Nourrit, and N. McLoughlin, "Dr hagnosis—a fundus image database for the automatic extraction of retinal surface vessels from diabetic patients," *Journal of Medical Imaging*, vol. 4, no. 1, pp. 014 503–014 503, 2017.
- [42] J. Staal, M. D. Abrámoff, M. Niemeijer, M. A. Viergever, and B. Van Ginneken, "Ridge-based vessel segmentation in color images of the retina," *IEEE Transactions on Medical Imaging*, vol. 23, no. 4, pp. 501–509, 2004.
- [43] J. Odstrčilik, R. Kolar, A. Budai, J. Hornegger, J. Jan, J. Gazarek, T. Kubena, P. Cernosek, O. Svoboda, and E. Angelopoulou, "Retinal vessel segmentation by improved matched filtering: evaluation on a new high-resolution fundus image database," *IET Image Processing*, vol. 7, no. 4, pp. 373–383, 2013.
- [44] J. I. Orlando, J. Barbosa Breda, K. Van Keer, M. B. Blaschko, P. J. Blanco, and C. A. Bulant, "Towards a glaucoma risk index based on simulated hemodynamics from fundus images," in *MICCAI*. Springer, 2018, pp. 65–73.
- [45] A. Sarhan, J. Rokne, R. Alhaji, and A. Crichton, "Transfer learning through weighted loss function and group normalization for vessel segmentation from retinal images," in *ICPR*. IEEE, 2021, pp. 9211–9218.
- [46] A. A. Ardakani, A. Mohammadi, M. Mirza-Aghazadeh-Attari, and U. R. Acharya, "An open-access breast lesion ultrasound image database: Applicable in artificial intelligence studies," *Computers in Biology and Medicine*, vol. 152, p. 106438, 2023.
- [47] S. Hesarakı, "Breast ultrasound images dataset(busi)," 2023. [Online]. Available: <https://www.kaggle.com/datasets/sabahearakı/breast-ultrasound-images-dataset>
- [48] A. Iqbal and M. Sharif, "Memory-efficient transformer network with feature fusion for breast tumor segmentation and classification task," *Engineering Applications of Artificial Intelligence*, vol. 127, p. 107292, 2024.
- [49] N. Vallez, G. Bueno, O. Deniz, M. A. Rienda, and C. Pastor, "Bus-uclm: Breast ultrasound lesion segmentation dataset," *Scientific Data*, vol. 12, no. 1, p. 242, 2025.
- [50] R. K. Saha, A. M. Chowdhury, K.-S. Na, G. D. Hwang, Y. Eom, J. Kim, H.-G. Jeon, H. S. Hwang, and E. Chung, "Automated quantification of meibomian gland dropout in infrared meibography using deep learning," *The Ocular Surface*, vol. 26, pp. 283–294, 2022.
- [51] L. Li and K. Xiao, "Children and adolescents meibomian glands (camg) dataset," 2024.
- [52] D. Vázquez, J. Bernal, F. J. Sánchez, G. Fernández-Esparrach, A. M. López, A. Romero, M. Drozdal, and A. Courville, "A benchmark for endoluminal scene segmentation of colonoscopy images," *Journal of Healthcare Engineering*, vol. 2017, no. 1, p. 4037190, 2017.
- [53] J. Bernal, F. J. Sánchez, G. Fernández-Esparrach, D. Gil, C. Rodríguez, and F. Vilarıño, "Wm-dova maps for accurate polyp highlighting in colonoscopy: Validation vs. saliency maps from physicians," *Computerized Medical Imaging and Graphics*, vol. 43, pp. 99–111, 2015.
- [54] J. Bernal, J. Sánchez, and F. Vilarino, "Towards automatic polyp detection with a polyp appearance model," *Pattern Recognition*, vol. 45, no. 9, pp. 3166–3182, 2012.
- [55] S. A. Hicks, D. Jha, V. Thambawita, P. Halvorsen, H. L. Hammer, and M. A. Riegler, "The endotect 2020 challenge: evaluation and comparison of classification, segmentation and inference time for endoscopy," in *ICPR*. Springer, 2021, pp. 263–274.
- [56] J. Silva, A. Histace, O. Romain, X. Dray, and B. Granado, "Toward embedded detection of polyps in wce images for early diagnosis of colorectal cancer," *International Journal of Computer Assisted Radiology and Surgery*, vol. 9, no. 2, pp. 283–293, 2014.
- [57] Q. Liu, C. Chen, J. Qin, Q. Dou, and P.-A. Heng, "Feddg: Federated domain generalization on medical image segmentation via episodic learning in continuous frequency space," in *CVPR*, 2021, pp. 1013–1023.
- [58] L. Jingxin, D. Qian, S. Linlin, L. Yuexiang, and Z. Yanfei, "Cross-organ and cross-scanner adenocarcinoma segmentation challenge," 2024. [Online]. Available: <https://cosas.grand-challenge.org/>
- [59] Z. Zhang, E. Keles, G. Durak, Y. Taktak, O. Susladkar, V. Gorade, D. Jha, A. C. Ormeci, A. Medetalibeyoglu, L. Yao *et al.*, "Large-scale multi-center ct and mri segmentation of pancreas with deep learning," *Medical Image Analysis*, vol. 99, p. 103382, 2025.
- [60] C. Martín-Isla, V. M. Campello, C. Izquierdo, K. Kushibar, C. Sendra-Balcells, P. Gkontra, A. Sojoudi, M. J. Fulton, T. W. Arega, K. Punithakumar *et al.*, "Deep learning segmentation of the right ventricle in cardiac mri: the m&ms challenge," *IEEE Journal of Biomedical and Health Informatics*, vol. 27, no. 7, pp. 3302–3313, 2023.
- [61] S. Bakas, S. Pati, M. Sheller, A. Karargyris, P. Mattson, B. Edwards, U. Baid, Y. Chen, R. T. Shinohara, J. Martin, B. Menze, M. Zenk, K. Maier-Hein, R. Floca, A. Reinke, L. Maier-Hein, F. Isensee, D. Zimmerer, and Y. Chen, "The federated tumor segmentation (fets) challenge 2022," Mar. 2022. [Online]. Available: <https://doi.org/10.5281/zenodo.6362409>
- [62] Z. Wang, F. Yi, P. Gong, C. He, C. Jin, and W. Zhang, "Population normalization for federated learning," in *CVPR*, 2025, pp. 10 214–10 223.
- [63] D. P. Kingma and J. Ba, "Adam: A method for stochastic optimization," in *ICLR*, 2015.
- [64] O. Ronneberger, P. Fischer, and T. Brox, "U-net: Convolutional networks for biomedical image segmentation," in *MICCAI*. Springer, 2015, pp. 234–241.
- [65] J. Chen and Y. Yuan, "Decentralized personalization for federated medical image segmentation via gossip contrastive mutual learning," *IEEE Transactions on Medical Imaging*, vol. 44, no. 7, pp. 2768–2783, 2025.
- [66] D. J. Farnell, F. N. Hatfield, P. Knox, M. Reakes, S. Spencer, D. Parry, and S. P. Harding, "Enhancement of blood vessels in digital fundus photographs via the application of multiscale line operators," *Journal of the Franklin institute*, vol. 345, no. 7, pp. 748–765, 2008.
- [67] J. Zhang, B. Dashtbozorg, E. Bekkers, J. P. W. Pluim, R. Duits, and B. M. ter Haar Romeny, "Robust retinal vessel segmentation via locally adaptive derivative frames in orientation scores," *IEEE Transactions on Medical Imaging*, vol. 35, no. 12, pp. 2631–2644, Dec 2016.
- [68] M. Antonelli, A. Reinke, S. Bakas, K. Farahani, A. Kopp-Schneider, B. A. Landman, G. Litjens, B. Menze, O. Ronneberger, R. M. Summers *et al.*, "The medical segmentation decathlon," *Nature Communications*, vol. 13, no. 1, p. 4128, 2022.
- [69] D. Jha, P. H. Smedsrud, M. A. Riegler, P. Halvorsen, T. de Lange, D. Johansen, and H. D. Johansen, "Kvasir-seg: A segmented polyp dataset," in *MMM*. Springer, 2020, pp. 451–462.
- [70] M. H. Yap, G. Pons, J. Martı, S. Ganau, M. Sentis, R. Zwiggelar, A. K. Davison, and R. Martı, "Automated breast ultrasound lesions detection using convolutional neural networks," *IEEE Journal of Biomedical and Health Informatics*, vol. 22, no. 4, pp. 1218–1226, 2017.